




A review on the role of interface in mechanical, thermal, and electrical properties of polymer composites

Marjan Alsadat Kashfipour¹ · Nitin Mehra¹ · Jiahua Zhu¹ 

Received: 15 November 2017 / Accepted: 22 January 2018 / Published online: 26 February 2018
© Springer International Publishing AG, part of Springer Nature 2018

Abstract

Composite materials and especially polymer composites are widely used in daily life and different industries due to their vastly different properties and design flexibility. It is known that the properties of the composites are strongly related to the properties of its constituents. However, it has been reported in many studies, experimentally and by simulations, that the characteristics of the composites do not follow the rule of mixing. It means that in addition to properties of the constituents, there are other parameters affecting the final physicochemical properties of composites. The interfacial interactions between fillers and host is one of the factors which can strongly affect the properties of the composite. In this review, we summarized the type of interactions between the constituents, their improvement techniques, interaction measurement methods, and the effects of interfacial interactions on thermal, mechanical, and electrical properties of composites.

Keywords Interface · Composites · Thermal conductivity · Mechanical strength · Electrical conductivity

1 Introduction

Polymers are molecules made of long chains of repeated units known as monomers. Their intrinsic features of flexibility, light-weight and low production cost, allow them to have wide applications in our daily life such as food packaging, painting, and automobile industries, etc. Although the monomer structure and selection of polymerization methods allow good control on some of the polymer properties, certain functions cannot be achieved by polymer itself. Therefore, polymers are compounded with other additives to achieve new properties. This final product is called composite [1].

Polymer nanocomposites (PNCs) are defined as the polymer matrixes reinforced with fillers with at least one dimension within 100 nm range. Nanofillers can be categorized based on their dimensions, e.g. 0D particle, 1D tube/fiber, and 2D sheets [2]. The PNCs have attracted great attention due to their drastically enhanced properties

[3–5]. For instance, thermally insulating polymers can be transformed into thermal conductors after reinforcing with carbon nanotubes (CNTs) [6–8]. Moreover, PNCs have demonstrated improved mechanical, gas barrier, solvent resistance, and flammability properties compared to the corresponding neat matrices [3, 4, 9]. The significant differences in properties of PNCs can be explained by the extremely large interface area of nanofiller. The interfacial area of nanofillers is orders of magnitude higher than traditional macro- or micron-sized additives [10, 11]. Therefore, the dispersion quality of nanofillers in polymer matrix becomes critically important. The techniques of incorporating nanofillers, dispersion control, and their impacts on the physicochemical properties of PNCs have been reviewed broadly [12–15].

Although the type and chemistry of the nanofillers are important for the prediction of their composite properties, the experimental and modeling results have not completely been in compliance with the predicted behavior. Therefore, there should have been other parameters which have either underestimated or not been considered in the prediction of composite behavior. In this regard, the interfacial interaction between polymer matrix and nanofiller became one of the parameters which have raised attention [16–19]. The presence of nanofillers in the matrix and their interfacial interaction can affect the mobility of polymer chains [20]. At high filler

✉ Jiahua Zhu
jzhu1@uakron.edu

¹ Intelligent Composites Laboratory, Department of Chemical and Biomolecular Engineering, The University of Akron, Akron, OH 44325, USA

content (over threshold), they can form a network which further restrains the mobility of the polymer chains [21]. Moreover, it has been reported that the property enhancement of polymer matrix filled with nanoparticles is a function of inter-filler distance, interfacial interactions, and interfacial area [22]. Hence, in addition to the characteristics of the constituents of the composites, the properties such as their interfacial areas, play a key role in the overall performance of composites. In this review, we described the type of interactions between the constituents, interaction characterization, improvement techniques, and the effect of interfacial interactions on thermal, mechanical, and electrical properties of PNCs.

2 Interfacial interactions in PNCs

The involved interactions in PNCs can be categorized into filler-filler and filler-polymer interactions. For instance, the interaction between the nanofillers (in the filler bundles) [23] or between different shells of the nanofillers such as multiwalled carbon nanotube (MWCNT) [24] is only related to the fillers and their properties. While the interaction between filler and polymer matrix [25] depends on the properties of both. The “interface/interphase” is defined as the region where the filler and matrix are either chemically or physically attached to each other [26]. A schematic model for the interface of filler in polymer matrix is shown in Fig. 1. The interfacial bonding plays a key role in polymer chain mobility and transferring the forces from the surrounding matrix to the filler. Therefore, it affects the mechanical properties of the polymer composites [17]. Following, the attributes of the fillers influencing the interfacial interactions, types of interfacial interactions, and the modification methods are reviewed.

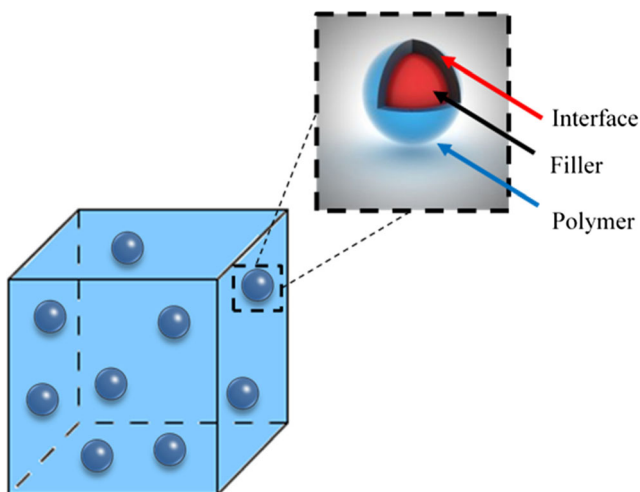


Fig. 1 Schematic model for the filler interface in a polymer composite

2.1 Effect of filler surface chemistry

Surface chemistry of the fillers can impact the filler-matrix and filler-filler interactions as well as the isotropic dispersion of fillers in the matrix. Stronger interfacial interaction between the composite constituents than the inter-filler interactions can lead to a better isotropic distribution [27, 28]. The inter-filler interaction is the reason for potential agglomeration of fillers. If the inter-filler interaction is highly attractive, the fillers can accumulate and then act as a bigger reinforcing cluster rather than individual particles. However, in the case of weak inter-filler interaction, the deformation of the aggregated fillers will affect the storage/loss of applied energy [28].

2.2 Effect of filler size and shape

As discussed earlier, the high surface to volume (SV) ratio of nanofillers is responsible for the significantly enhanced properties. Therefore, it can be counted as the primary motivation for nanocomposite development [28, 29]. This parameter in addition to the stress transfer [28, 30] is responsible for “new structural arrangement” at microscale in the composites. As a result, improving the interfacial regions can increase the chance of introducing new properties to the composites [28]. Based on Eq. (1), SV ratio of spherical fillers is a function of $(1/r)$:

$$\frac{A_s}{V_s} = \frac{4 \cdot \pi \cdot r^2}{\frac{4}{3} \cdot \pi \cdot r^3} = \frac{3}{r} \quad (1)$$

where A_s is the available surface area, V_s is the volume of the filler, and r stands for spherical radius. To investigate the effect of the interfacial area, the whole interfacial area involved in the composites should be considered. For this purpose, in addition to surface volume ratio of individual fillers, the volume fraction (φ) of the fillers should be considered as well (Eq. (2)):

$$\frac{A_{\text{total}}}{V_{\text{total}}} = \frac{3}{r} \cdot \varphi \quad (2)$$

where A_{total} is the total surface area of the fillers and V_{total} is the total volume occupied by the fillers. Therefore, the overall surface to volume ratio is a function of $(1/r)$ and φ . This means that in a constant volume fraction, by decreasing the size of fillers, the overall interfacial area will be increased and followed by increment of the interfacial interactions. As a result, the interfacial stress transfer will be more efficient. Additionally, for a specific size of fillers, by increasing the content of filler in the composite, the interfacial regions can be increased as well.

For cylindrical fillers, this ratio can be expressed in Eq. (3):

$$\frac{A_c}{V_c} = \frac{2 \cdot \pi \cdot r^2 + 2 \cdot \pi \cdot r \cdot L}{\pi \cdot r^2 \cdot L} = \frac{2}{r} + \frac{2}{L} \quad (3)$$

Comparing the spherical and cylindrical shaped fillers, their SV ratio can be expressed in Eq. (4):

$$\frac{SV_s}{SV_c} = \frac{3}{2 \cdot (1 + r/L)} \quad (4)$$

Hence, for plates ($r > L$) and short rods ($L < 2r$) the SV ratio of cylindrical fillers is larger than spherical fillers', while the SV ratio of long fibers ($L > 2r$) is smaller than the spherical filler. Although it seems that due to high SV ratio of cylindrical fillers, it is better to use them as reinforcing agents, but there are other factors that may influence the selection of filler shape. For example, rigid cylindrical fillers can hardly disperse isotropically at high concentrations [28]. For thermal conduction, composites with smaller fillers (larger interfacial area) have severe phonon scattering resulting in lower thermal conductivity (TC) [31]. For example, Wu et al. investigated the effect of graphite nanoplatelet size (1 to 15 μm) on thermal conductivity of polyetherimide (PEI) composites. It was shown that although the smaller particles formed a better network, the thermal conductivity of the composites was higher with larger particles. It was suggested that the interfacial thermal resistance is the dominant parameter that determines the TC of the composites [32]. Eventhough larger enhancement of TC was also reported in other composites with larger fillers [33, 34], there are some contradictory reports as well [35, 36]. For instance, Pashayi et al. found that nano-sized silver particles outperformed micron-sized particles in enhancing TC of epoxy-silver composites. SEM observations revealed that nano-sized fillers formed a continuous network which was not observed for micron-sized fillers [37]. However, it is known that TC is not only a function of particle size; other parameters such as surface chemistry, morphology, and dispersion of fillers could affect TC as well. Therefore, more likely, the effect of size should be discussed with other parameters when interpreting the thermal conduction in polymer composites [38]. Fu et al. reported higher TC for epoxy adhesives filled with nano-sized Al_2O_3 compared with micron-sized filled ones. The authors believed that higher polydispersity of nano-sized fillers helped to construct an effective filler network for heat transfer [36]. In contrary to high interfacial thermal resistance in polymer nanocomposites, combination of nanoparticles with microparticles could synergistically enhance the TC of composites. This phenomenon has been observed in several systems, which was attributed to bridging effect of nanofillers between micron-sized fillers [36].

With filler size down to nanometer, the SV ratio and surface energy of nanofillers become large enough that lead to a

dramatic change in physicochemical properties of PNCs due to the presence of large interface area between filler and polymer matrix. It should be also considered that homogenous dispersion of the nanofillers is essential for achieving the desired mechanical properties.

In terms of stiffness, the effect of filler size seems more complicated. It was reported that the size of fillers in a constant volume fraction cannot significantly affect the stiffness (or called Young's modulus) [39, 40]. However, Ji et al. have theoretically proved that there is a critical size for fillers in nylon 6/montmorillonite nanocomposites, below which the filler size can affect the stiffness (Fig. 2) [41]. This phenomenon has been experimentally proved in separate studies [42, 43]. Therefore, the stiffness of the composites can be either unaffected or decreased by increasing the filler size [44].

2.3 Types of interfacial interactions

The properties of the composite materials are framed based on the interfacial characteristics of the fillers and matrixes [45, 46]. Generally, the interactions between the filler and matrix are categorized as covalent and noncovalent interactions (i.e., van der Waals (VDW) [45], electrostatic [45], and hydrogen bonding [47–49]). Depending on interactions between the constituents of the composite, different types of improvement techniques were developed [16].

2.3.1 Noncovalent interaction

The noncovalent interaction between the matrix and fillers can be enhanced by employing bridging, increment of interfacial area, and polymer wrapping [16]. Bridging happens when a polymer chain interacts with two or more reinforcing fillers simultaneously (Fig. 3). The probability of the presence of bridging in the composite depends on the ratio of the radius of gyration (R_g) of the polymer chain to the average distance

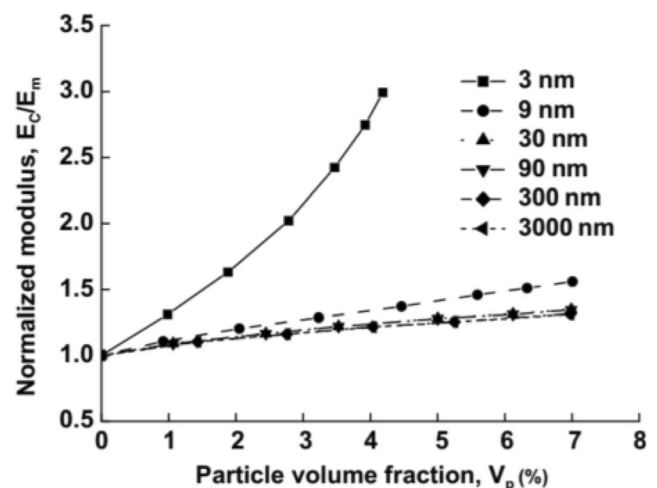


Fig. 2 Normalized modulus as a function of particle size [41]

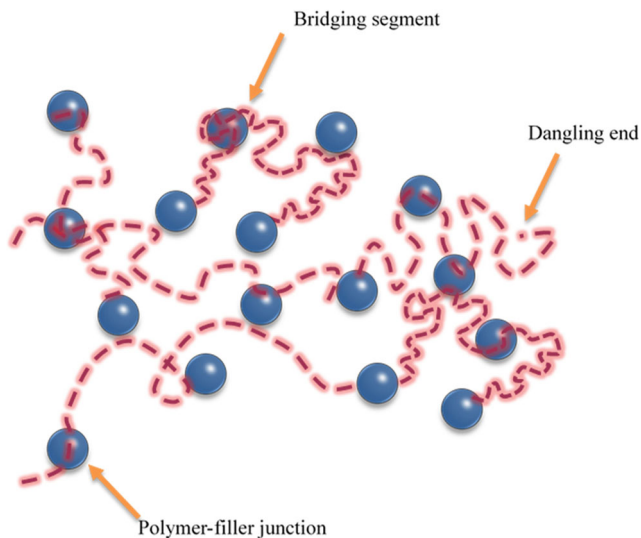


Fig. 3 Schematic drawing of bridging incident in polymer composites

of nearest reinforcing filler. Therefore, by increasing the filler content and using higher molecular weight polymer, the chance of bridging phenomenon will be higher [50].

Specific interaction area in the composite is another factor which can affect the properties of the composite. It is defined as interfacial area of polymer-filler per unit volume and it is related to the density ratio of polymer matrix to the fillers, the concentration, and diameter of the filler [50]. In this regard, Cadek et al. have shown that the reinforcement of polymer composites is linearly related to the overall interfacial area of fillers, meaning that the smaller fillers can have higher impact on the property of the final product [29].

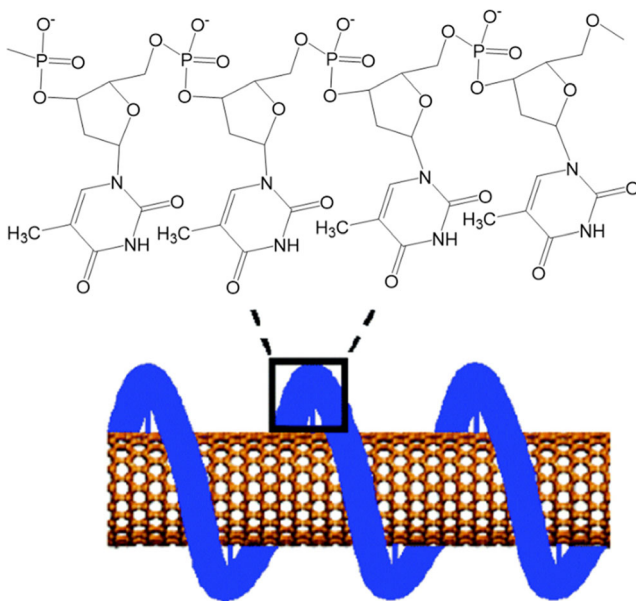


Fig. 4 Schematic drawing of a single wall CNT wrapped with DNA [63]

Wrapping fillers by polymer chains, in addition to increment of the interaction, is useful for better dispersion of the fillers in the matrix [51–54]. Wrapping of the nanotubes by the polymer chains has been explained by presence of π - π stacking [55–59], hydrophobic [60], and VDW interactions [61, 62]. Figure 4 shows the schematic of a wrapped single wall carbon nanotube (SWCNT) by DNA which is due to π - π stacking interaction between the SWCNT wall and the aromatic bases of DNA [63].

Wrapping fillers by polymer is related to the chemical composition and stiffness of the polymer backbone [60] and geometric parameters [50] of the constituents in the composites. Thus, higher molecular weight polymers and nanotubes with smaller diameters are more likely to go through the wrapping mechanism [16].

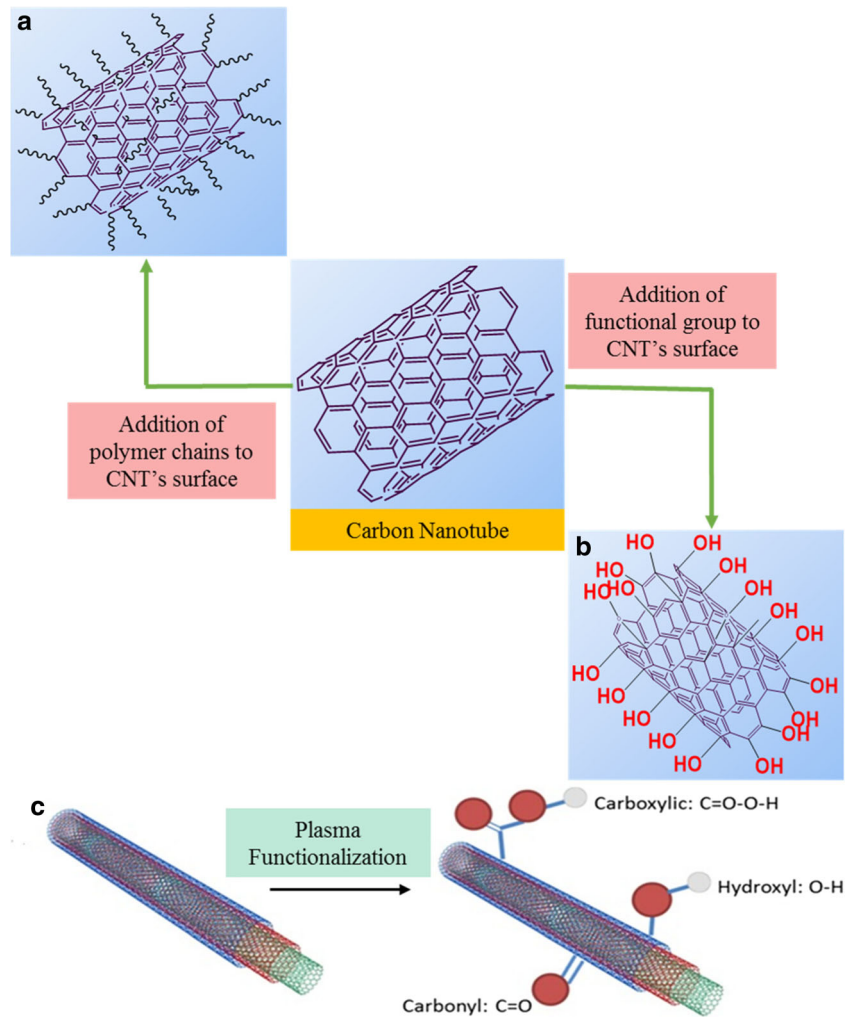
Finally, it should be noted that crystallization of the semi-crystalline polymer host at the interface is another way for improving the interfacial interactions. In this process, the fillers will act as a nuclei and the semi-crystalline host will crystallize at the interface [64].

2.3.2 Covalent interactions

Covalent interaction happens when polymer chains are chemically connected to the reinforcing fillers [16]. For that purpose, proper chemical treatments are required to attach functional groups to filler surface which can react with the matrix [65–70]. Figure 5a–c shows three types of surface functionalization of CNT with polymer chains, hydroxyl, and carboxyl groups, respectively. Functionalized fillers not only enhance their interaction with the host, but improve their dispersion and the final properties of the composites compared to the pristine fillers [71–73]. The functional group of the fillers should react with an active group on the polymer chains of the host. One of the suitable methods for chemical bonds formation is the in situ polymerization, where the monomers react with each other and the fillers simultaneously [74–78]. The other way is to modify the host prior to the chemical attachment of the fillers [79].

Although covalent bonding between the fillers and the host can enhance the interfacial strength more effectively (due to stronger adhesion), the involved pretreatment process requires special attention. For instance, even though the functionalized fillers could achieve better dispersion, but introduction of surface defects could deteriorate the intrinsic properties of the filler [16]. Grafting polymer chains on filler surface have been demonstrated effective approach to improve the interfacial interaction and thus enhanced property of the composites [80–82].

Fig. 5 a, b Schematic drawing of modification of CNT's surface by addition of polymer chains and functional groups, respectively. c Functionalization of multiwall CNT (MWCNT) by plasma functionalization [83]



3 Experimental methods of measuring interfacial interactions

3.1 Interfacial wetting properties

For strong adhesion between the fillers and matrix, good wettability of the reinforcements by the matrix is required [84], which makes it important to evaluate the wettability of the fillers. In the following section, contact angle [85] and surface tension [86] methods will be introduced for wettability measurement.

The concept of contact angle was first introduced by Thomas Young in 1805 [87]. He proposed that the contact angle of a drop of a liquid on a solid surface is the result of mechanical equilibrium between three surface tensions. The involved surface tensions at the interface are liquid/vapor (γ_{LV}), solid/vapor (γ_{SV}), and liquid/solid (γ_{LS}). This equilibrium results in the following Eq. (5) [88]:

$$\gamma_{SV} - \gamma_{SL} = \gamma_{LV} \cdot \cos\theta \tag{5}$$

This concept is important as the angle of the liquid drop at equilibrium state gives information on wettability and spreadability of the liquid on the solid surface [88]. The contact angle (θ) below 90° indicates that wetting is favorable while for angle above 90° ($\theta > 90^\circ$) is not (Fig. 6) [89]. In other words, the lower the angle, the better the wettability. Complete wetting can be achieved when contact angle approaches to 0° [90].

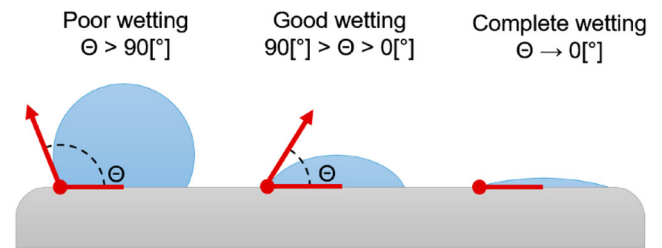


Fig. 6 The schematic presentation of the relationship between contact angle and wettability [89]

Contact angle measurements of the nanofillers with polymer matrixes have been studied in both microscopic and macroscopic scales [84]. For instance, the wetting property of carbon nanotubes in macroscopic scale was evaluated by placing the liquefied matrix (or the powder followed by applying heat to convert it to liquid) on the nanotube sample. The aim was to see whether the liquefied matrix would absorb (wetting contact angle) by the surface or it would make a spherical bead (nonwetting contact angle).

Further, using drop-on-fiber techniques [85] and characterization by scanning electron microscopy (SEM) [84], transmission electron microscopy (TEM) [86] and optical microscope [91], the shape and symmetry of the drop on the cylindrical fiber can be studied. In drop-on-fiber method, the drop will be symmetrically shaped along the cylindrical axis when the contact angle is zero, in contrast to the high contact angle which results in nonsymmetrical conformation [92, 93]. For instance, Qian et al. used the drop-on-fiber approach to evaluate the wettability of carbon fiber (CF) and its CNT-grafted version with poly (methyl methacrylate) (PMMA) as matrix (Fig. 7). The contact angle of CF changed from 27.4 ± 0.8 to $25.7 \pm 0.8^\circ$ after oxidation, while grafting CNT to CF resulted in further drop of the contact angle to $21.6 \pm 0.7^\circ$ [94].

Wetting property of the fibers at microscale has been studied with the Wilhelmy model [95, 96]. Combination of the Wilhelmy model with atomic force microscopy (AFM) makes it a useful technique for measuring the wetting properties of the carbon nanotubes. For this purpose, carbon nanotube will be attached to a calibrated AFM tip and will be brought down to immerse CNT in the polymer melt. This process will be followed by inducing a downward force on the CNT, which will be recorded by the cantilever deflection. The deflection force can be converted to the contact angle by knowing the surface tension of the liquid. The following Eqs. (6) and (7) will be used for this conversion:

$$F_r = \gamma_L \pi \cdot d \cdot \cos\theta \quad (6)$$

$$F_r = \gamma_L \cdot \pi \cdot (d_{\text{out}} \cdot \cos\theta_{\text{out}} + d_{\text{in}} \cos\theta_{\text{in}}) \quad (7)$$

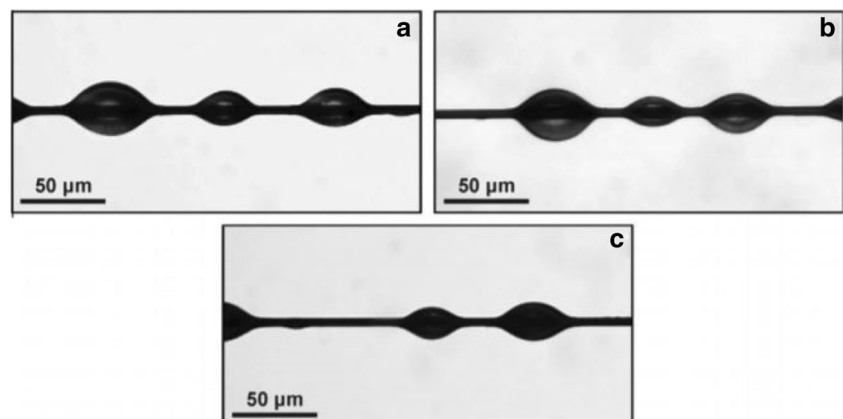
where γ_L is the surface tension of the liquid (N/m), θ is the contact angle in degree, θ_{in} and θ_{out} are the inside and outside contact angles of the nanotube, d is the diameter of the nanotube, and d_{in} and d_{out} are the inside and outside diameters of the nanotube [97–99].

Although the wetting measurements are known as simple method to estimate of the interfacial adhesion, significantly different values are reported even for the same materials. For example, the contact angle of PEG-MWCNT was reported to be in the wide range of $25\text{--}73^\circ$ in different studies. The difference between observed results could be explained by the different size of fillers and also temperature variations in the system [84, 99]. Therefore, these methods could provide an initial estimation for the recognition of strong or weak interactions [16]. Thereafter, researchers found surface tension measurement a better technique for wettability studies [84, 98]. In this method, the surface tension of the polymer will be compared with the critical surface tension of the nanotube (γ_c) (in the plot of $\cos\theta$ versus γ_L of various liquid, the intercept at $\cos\theta = 1$ shows the critical surface tension) [95]. In theory, liquids with surface tension equal or less than the critical surface tension of substrate (γ_c) can completely wet the surface [90].

3.2 Spectroscopy techniques

The spectroscopy techniques such X-ray diffraction, Raman, and Fourier transform infrared (FTIR) are well-known methods for material characterization. Raman spectroscopy was first conducted on CNTs in 1993, and since then, it has been used for characterization of nanocomposites [100]. Raman spectroscopy can be used for detection of the type of functionalization [101] and the diameter of the nanotubes [102, 103]. Furthermore, the chemical peak shifts in Raman/FTIR can be used to distinguish the VDW interactions between the nanotubes in the bundle [104, 105], the hydrogen

Fig. 7 Optical images of PMMA droplets on **a** as-received, **b** oxidized, and **c** CNT-grafted carbon fibers [94]



[106], and covalent bonding between the nanotubes and the polymer matrix [107].

3.3 Atomic force microscopy involved techniques

As mentioned earlier, recent developments in the force microscopy techniques makes it feasible to measure the force between the cantilever and the substrate even in atomic resolution [108] e.g. for measuring the interactions in the nanotube composites. Two major approaches have been developed for this purpose. In the first approach, a nanotube attached tip will be prepared and a polymer melt will be used as the substrate [97–99, 109] (similar to the contact angle measurement mentioned in previous section), while in the second approach, the tip will be coated with the polymer and the nanotube is placed as the substrate [110].

3.3.1 CNT-on-tip/cantilever approach

This approach involves two different methods for strength measurement: (i) pull out method [111] and (ii) peeling force microscopy method [112]. Figure 8 shows the pull out technique which was used by Barber et al. for the first time. Using this method, they could measure the critical force required for interfacial failure between CNT and a copolymer melt [113]. In the pull out method, the CNT attached tip will approach the polymer melt, while the applied force on the cantilever is simultaneously recorded as a function of time. When the tip is close enough to the polymer surface, a jump-in force is usually observed in the force curve. Afterwards, by pushing the CNT further into the bath and keeping it stationary for a while, the polymer will solidify around it and later will be pulled out from the matrix (Fig. 9). For this procedure, it is required to investigate the length and diameter of the nanotube after pull out process to see if any changes have occurred [111, 114, 115].

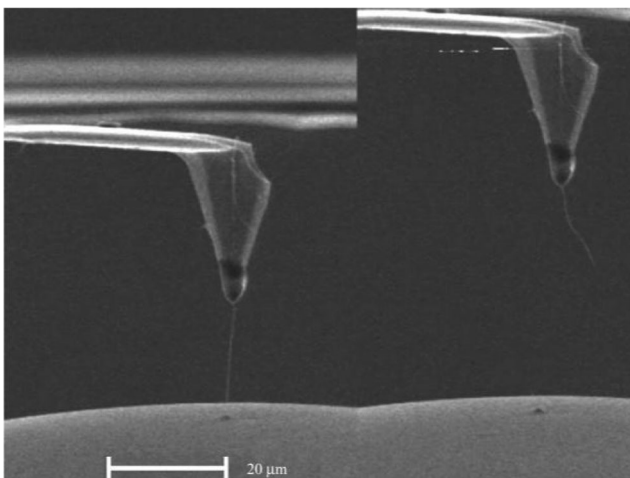


Fig. 8 CNT attached AFM tip is immersed in the resin followed by pulling out and measuring its required force simultaneously [113]

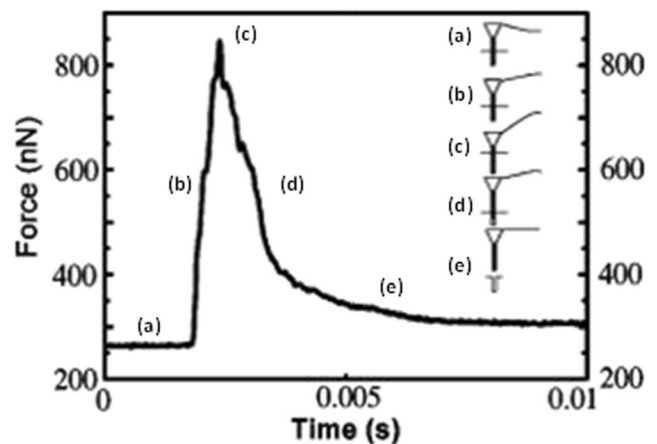


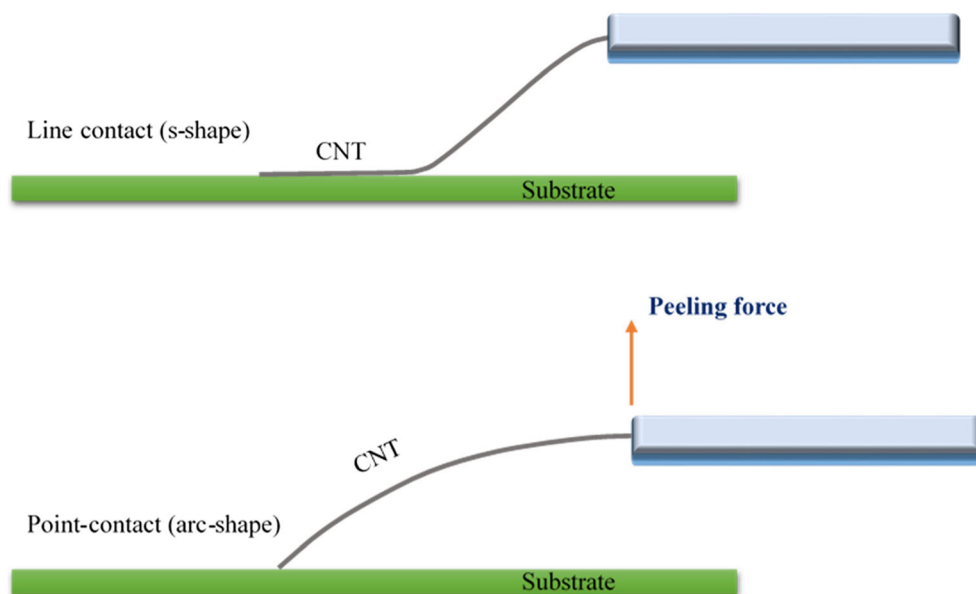
Fig. 9 Force vs. time plot for the pull out approach: **a** the nanotube is already in the polymer bath; **b** by pulling out the nanotube, the cantilever will be deflected until it reaches its maximum deflection at **c**. At **d**, the pull out is occurring, while at **e**, it is completely out of the bath [111]

The other method is the peeling force microscopy. In this method, the CNT is attached to a tipless cantilever and it will be in touch with the substrate. In next step, the nanotube will be peeled off from the surface, generating the force curve simultaneously. During this process, the nanotube will go through different geometrical configurations with regards to its contact with the substrate: line contact (s shape), point contact (arc shape), and finally no contact or freestanding mode (Fig. 10). Based on a proposed theoretical model, each of these configurations represent specific kind of involved energy in separating the nanotube from the substrate and the applied work in s-shape mode will mostly change the interfacial energies of constituents. Although this technique is useful for interaction measurement, it cannot measure the interfacial energy per unit area due to difficulty of measuring the contact area during this process [112, 116].

3.3.2 CNT-on-substrate approach

In contrast to the previous approach, CNT will be placed as the substrate, and a modified AFM tip (chemically modified either by applying the polymer as a coating or binding functional groups to it) will be used. Later, the force curve between the cantilever and the substrate will be recorded and used to measure the corresponding adhesion. This type of measurement is useful to show the effect of present chemical groups on the adhesion between the polymer matrix and the nanotubes [110, 117–120]. However, it worth mentioning that in this method only the maximum adhesion force will be considered, which is the summation of all forces applied on different locations of the cantilever. Therefore, the tip-substrate distance will influence the final value of the adhesion force. Recent studies have introduced a new parameter for measuring the adhesion force which is also a function of separation distance, called interaction stress. This parameter is “the state of stress (i.e., a tensor)

Fig. 10 The s-shape and arc-shape CNT configuration on the substrate [112, 116]



at any given point of an object as a result of its vicinity to a secondary object” [121]. In order to get this factor, a stepwise discretization method was applied to the force curve of AFM followed by determination of the noncovalent interactions versus separation distance. Furthermore, all the other interaction parameters can be calculated (e.g., interaction forces, energy and internal stress) from interaction stress as well [120, 121]. Additionally, each of these factors can be used for measuring the other parameters such as the stress field at nanoscale [121, 122].

4 Influence of interface on mechanical properties

It is known that incorporation of fillers in a matrix can modify its properties. In conventional composites, micrometer-sized inorganic fillers such as calcium carbonate, talc, and glass beads have been extensively used for mechanical property enhancement [123–125]. Such properties can be further improved by decreasing the fillers’ size to nanoscale and increasing their aspect ratio.

Since the behavior of PNCs is greatly influenced by their microstructures, the properties of matrix and fillers, filler distributions, interfacial bonding, and processing method should all be considered [123, 126]. Mechanical properties of composites are more related to particle size, loading, and filler-matrix interfacial adhesion [44]. The interfacial property is important for the evaluation of the mechanical load transfer from polymer matrix to fillers [127, 128]. For instance, strength and toughness of the composites strongly depend on the interfacial adhesion. Therefore, the dispersion, interfacial adhesion, geometric dimensions, etc., play key

roles in mechanical property enhancement [76, 129–131]. The mechanical properties can be evaluated by either conventional methods such as dynamic mechanical analysis (DMA) [27, 132]; tensile, compression, and shear tests [25, 133–135]; or the new methods such as copper grid technique [136, 137] and strain-induced elastic buckling instability for mechanical measurements [138–140]. Since stiffness is not significantly affected by the degree of interfacial bonding in polymer composites [141, 142], it is not reviewed here.

4.1 Strength

The tensile strength of the composite depends on the efficiency of stress transfer between the constituents of the composite. If the applied load efficiently transfer to the fillers, the strength will be improved [143, 144]. The smaller particles have larger interface area at a constant volume fractions of fillers, leading to a large portion of stress transfer regions [44].

The efficiency of the load transfer also depends on the strength of interfacial bonding between the composite constituents [44, 145]. Contrary to the composites with strong interfacial interaction [142], strength will be decreased in composites with poorly bonded fillers. This is due to the presence of discontinuity because of de-bonding at the interface, which prevents the filler from carrying the applied load efficiently. There are many studies on filler surface modification that lead to higher dispersion and interfacial interaction and subsequently higher tensile strength of the composites [76, 146–149]; suggesting that, the introduction of chemical bonding to filler-matrix interfaces can effectively enhance the strength of composites [150, 151].

An et al. incorporated functionalized rod-shaped silicates known as attapulgite (ATT) into the polyimide (PI) films. For that the fillers' surface was grafted with polymer chains similar to the matrix. The functionalization of the silicates resulted in better dispersion of ATT and more efficient stress transfer between filler and matrix. The final composite showed an increase of 70% in tensile modulus, 45% in tensile strength, and 54% in elongation at break. The enhanced mechanical properties were explained by considering the predominant factors such as the percolated particle networks, interfacial interactions, and introduced free volume due to addition of the fillers. The enhanced properties were induced at three different stages: (i) at low concentration of fillers, the reinforcement was due to interfacial interactions, leading to effective stress transfer between fillers and matrix; (ii) after reaching the percolation threshold, in addition to the interfacial interactions, percolated particle network also enhanced the strength of the composite; (iii) further increasing the fillers' concentration beyond percolation increases free volume and decreases the tensile strength by crack initiation and propagation. Therefore, depending on the concentration of reinforcing agents in the composite, the mechanical properties could be enhanced by interfacial interaction, percolated network, or both of them. At high loading degrees, the strength will be decreased due to crack formations [152]. Results mentioned above, are consistent with other studies stating that the addition of nanoplatelets into the polymer matrixes can improve their stiffness and toughness and possibility of de-bonding at the interfaces at high volume fraction of the fillers [153].

In addition to the surface modification of fillers, interfacial crystallization can also enhance the interfacial interactions followed by more load transfer. The mechanism of such mechanical property enhancement has been systematically studied and been explained by: (i) improvement of interfacial interactions in the filler/crystalline polymer compared to the filler/amorphous polymers, (ii) crystalline phase of polymer acts as an additional stiff constituent in the composite, and (iii) reduction of filler aggregation due to the formation of crystalline phase at the boundaries [64, 154].

4.2 Toughness

The role of nanofillers in development of tough polymeric products have been reported [155, 156]. However, the enhancement of the strength of composites are accompanied with sacrificing toughness of the products [157]. Likewise, toughening agents such as rubbers which are used to enhance the extensibility and the fracture resistance of polymers, reduce the strength of product [158, 159]. Therefore, the balance between these two properties should be considered when designing desired properties in composites [160, 161]. The fracture behavior of polymer nanocomposites which defines their toughness is a function of the type of polymeric matrix [44],

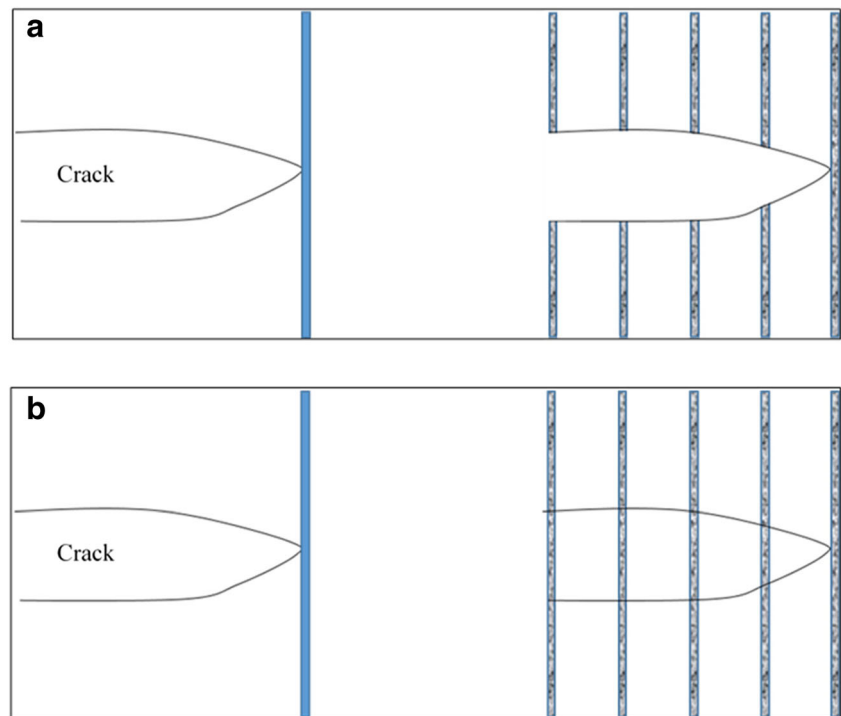
size and shape of fillers [152], and the interfacial interactions [152]. For instance, toughness can be significantly enhanced by the enhancement of the interfacial adhesion between the thermoplastic matrix and filler; but not in composites with thermosetting matrix [44]. Yet, the simultaneous enhancement of toughness and strength in glassy polymeric matrix is unclear [152].

Sakai et al. investigated the mechanical properties of brittle carbon matrix reinforced with carbon fiber. They proposed that if inappropriate interaction was embedded between the components, the cracking of matrix would propagate along the fibers. In that case, the fibers could not bridge the crack and lead to weak toughening of the composite. On the other hand, for the interactions which were strong enough for stress transfer and weak for de-bonding to happen, the crack pattern changed significantly (crack deflection, voiding, and de-bonding). This phenomenon resulted in fiber pull out followed by bridging the crack and toughening the composite (Fig. 11) [162]. Boo et al. studied the exfoliated epoxy/ α -zirconium phosphate nanocomposite. They claimed that since fillers had strong bonding with the matrix, no crack blunting and deflection occurred. The crack went through fillers by breaking them; thus, there was no improvement in toughness [163].

Moloney et al. also reported that though epoxy/glass bead composite had a low strength due to the poor bonding and the toughness was enhanced due to crack tip blunting [159, 164]. Similarly, Liu et al. explained the toughening of intercalated epoxy/clay nanocomposite due to the crack deflection and de-bonding process. The toughness of epoxy resin was enhanced by 70% after adding 4 wt% of clay [165]. The same result was reported by Zuiderduin et al. for toughening of aliphatic polyketone by stearic acid-coated calcium carbonate particles. They claimed that rigid particles can enhance the toughness of composites with reduction of the volume strain. That required the particles to de-bond from the host [166]. For this mechanism to happen, fillers should have a round shape (no stress concentration) and their size should be less than 5 μm (in this study, it was around 0.7 μm ; otherwise, the created voids would cause fracture initiation), well dispersity of fillers, and moderate interfacial interactions. The stearic acid coating used in this study was for enhancing the dispersion of the particles and lowering the interaction with the matrix. Thus, due to de-bonding mechanism, the toughness of the composite was increased [166, 167]. On the other hand, Levita et al. believed that at high enough adhesion between the filler and the matrix, the crack will be arrested (pinned) by reaching the filler (known as crack pinning model). Further propagation of the crack, needed higher tension. It was mentioned that the size of the filler was important to be able to interact with the crack [168].

Fiedler et al. investigated the effect of CNT on the toughness of epoxy composites. They showed that although

Fig. 11 Crack interaction with fibers for **a** strong and **b** weak interactions [162]



untreated CNT could enhance the toughness due to void nucleation and crack deflection, the amino-functionalized carbon nanotube had a better performance. The fracture toughness of the resin was enhanced 45% by incorporation of just 0.3% of amino-functionalized double-walled CNT. They concluded that crack bridging by fiber can further enhance the toughness of composites [169]. Gojny et al. summarized the possible fracture mechanisms of CNT-filled composites as shown in Fig. 12 [170]. Table 1 briefly summarizes the change of mechanical properties of polymer composites after introducing different fillers. To sum up, depending on the dominant toughening mechanism and the type of matrix (thermoplastic vs. thermoset), higher interfacial interaction may have positive or negligible impacts on the toughness of composites.

5 Influence of interfacial interactions on thermal properties

Investigation of the thermal behavior of nanocomposites is essential for determining the applicable temperature range of the materials [180]. In this section, we will review the effect of fillers and proximity to the fillers' surfaces on the thermal properties of composites, such as glass transition, thermal stability, and interfacial thermal resistance.

5.1 Glass transition (T_g)

The impacts of the size and confinement on the glass transition and dynamics of polymer chains at the interface have

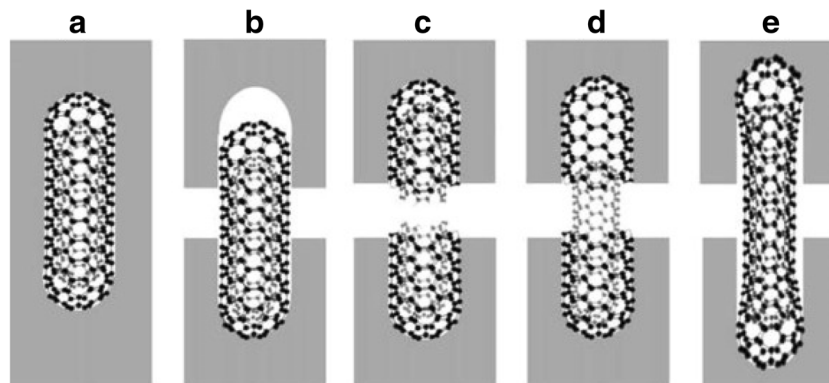


Fig. 12 Schematic representation of fracture mechanisms of CNT-filled composites. **a** Initial position of CNT in a matrix. **b** CNT-pull out as a result of CNT-polymer debonding (weak interfacial interaction). **c** CNT's rupture which is caused by strong interfacial adhesion and fast local

deformation. **d** Telescopic pull out resulting in outer layer fracture (due to strong adhesion) and inner layer pull out. **e** Crack bridging phenomenon combined with partial debonding [170]

Table 1 Mechanical property of polymer composites with different fillers and bonding types

Filler	Fraction	Matrix	Bonding type	Property	Changes	Ref.
Silica	20 vol%	Epoxy	VDW	Strength	Decreased	[159]
Polymer-coated CNF	0.8 wt%	Epoxy	H-bonding, covalent bonding	Strength	+ 10.5%	[49]
Silica nanoparticles	13.4 vol%	Epoxy	VDW	Toughness	Improved	[161]
ZrP nanoplatelets	2 vol%	Epoxy	VDW	Toughness	No change	[163]
Organoclay	4 wt%	Epoxy	VDW	Toughness	+ 27%	[165]
GA-II/graphene (noncovalent)	2 wt%	Epoxy	Improved interaction	Strength	+ 70%	[171]
Amino-functionalized double-walled CNT	0.3 wt%	Epoxy	Covalent bonds	Toughness	+ 45%	[169]
Functionalized CNT	10 wt%	Nylon 6	Improved interaction	Strength	126%	[172]
Polymer-functionalized MWCNT	0.3 wt%	Poly(vinylidene fluoride) (PVDF)	Improved interaction	Strength	+ 90%	[173]
SWCNT	0.4 wt%	Poly(ethylene terephthalate) (PET)	Covalent bonds	Strength	+ 16%	[174]
SWCNT	1.0 wt%	Polyurethane (PU)	Both noncovalent and covalent bonding	Strength	+ 50%	[175]
Chlorinated polypropylene (CPP)-grafted MWCNT	0.6 vol%	CPP	Improved interaction	Strength Toughness	+ 280% + 300%	[176]
CPP-grafted MWCNT	0.5 wt%	Polystyrene (PS)	Improved interaction	Strength	+ 100%	[133]
(PS-co-PCMS)-b-PS Functionalized SWCNTs ^a	0.06 wt%	PS	Improved interaction	Strength	+ 82%	[177]
Graphene nanoplatelet (GNP)-5	5 wt%	Epoxy	VDW	Strength	~ - 60%	[178]
Noncovalent functionalized graphene flakes	0.25 wt%	Epoxy	Improved interaction	Strength	+ 75%	[179]

^a Copolymers of styrene and *p*-chloromethylstyrene

been reviewed earlier. Evidence of the effect of interface has been found on the variations of the glass transition temperature or the dynamics of molecules [20, 181, 182]. Presence of reinforcing particles in the polymers can affect the local segmental mobility of polymer chains. This parameter can be evaluated either by measuring the segmental relaxation time or the T_g behavior before and after filler addition [20]. The relaxation time was mainly measured using dielectric spectroscopy [183, 184], NMR spectroscopy [185–192], and neutron scattering [193, 194]. T_g was determined using dynamic mechanical spectroscopy [195–199], calorimetry [191, 200–202], and dilatometry [184, 203] techniques. Since the mobility of the polymer chains around the fillers is related to the interfacial interaction, the presence of the interaction and their strength can be estimated by measuring T_g and relaxation time [11, 204]. For example, stronger interactions will cause reduction of the dynamic loss, decrement of thermal expansion coefficient and increment of T_g [205]. On the other hand, in NMR measurements, bonding strength between the polymer chains and the filler particles show different relaxation times [185].

For different polymer nanocomposites, T_g was shown to be increased [206, 207], decreased [180, 208], or even unaffected [182, 209] by the introduction of fillers into the system. More studies are summarized in Table 2.

The presence of strong interaction between the matrix and the fillers (e.g., H-bonding [30, 220], electrostatic interaction [220, 221], and covalent bonding [222]) increase the T_g while the free space at the interface of nonwetted fillers lead to reduced T_g [204, 223]. The absence of strong interfacial interaction of wetted fillers have no substantial impact on T_g [182, 204]. This phenomenon was explained by the thermomechanical similarities of planar polymer films and polymer nanocomposites [223]. If the interaction between the fillers and surrounding matrix is the same as the interfacial interaction between ultrathin layer of the bulk polymer and the substrate, T_g will be invariant [204]. Additionally, it was reported that there may be more than one T_g in polymer nanocomposites with strong interactions between the fillers and polymer chains [196]. In that case, higher T_g belongs to the regions adjacent to the fillers with irreversible adsorption of polymer chains to the particles, while the lower T_g represents for the polymer bulk farther from the fillers [182]. It should be mentioned that different T_g values have been reported for the same materials, which can be the result of incorporating different methods of analysis [20], neglecting the effect of fillers on the degree and nature of crystallinity of the matrix [20], or different methods of preparation [224].

Table 2 Glass transition behavior of polymer composites after incorporation of fillers

Filler	Fraction	Matrix	T_g change (°C)	Ref.
Alumina	1.0 wt%	PMMA	-25	[180]
Mica	3 wt%	Poly(butylene terephthalate)	+6	[210]
Exfoliated clay (MMT)	< 10 wt%	Poly(vinyl chloride)	-1 to -3	[211]
Nanoclay	2.5–15.1 wt%	PMMA	+4 to +13	[212]
Nanoclay	4 wt%	Poly(propylene carbonate)	+13	[213]
Nanoclay	6 wt%	Natural rubber	+3	[214]
Nanoclay	5 wt%	PS	+6.7	[215]
Noncovalent functionalized graphene flakes (GFs)	10 wt%	Epoxy	+6.7	[216]
Diglycidyl ether of bisphenol A-functionalized GO (DGEBA-f-GO)	0.5 wt%	Epoxy	+3.9	[179]
Alumina	4.0 vol%	Poly(2-vinyl pyridine)	+16	[204]
	4.0 vol%	PS	No change	
Silica	2.0 wt%	PET	+10	[206]
Functionalized SWCNT	1.5 wt%	PS	+3	[217]
SiC	0.5–1.5 wt%	Polycarbonate (PC)	No change	[218]
Unmodified MWCNT	6.98 wt%	PI	-4.59	[219]
Acid modified MWCNT			+2.97	
Amine modified MWCNT			+4.75	

5.2 Thermal stability

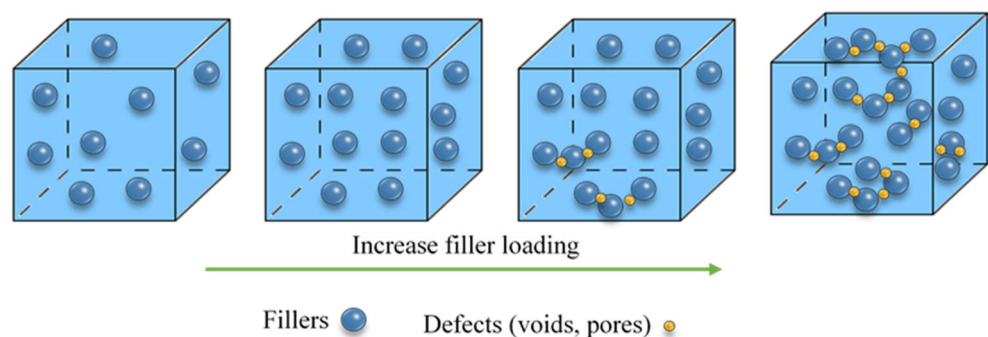
The improved thermal stability of the PMMA/montmorillonite PNCs was first reported by Blumstein in 1965 [225]. Higher thermal stability and improved flammability performance make them suitable for high-temperature applications. Additionally, since many of the polymer composites are produced through melt mixing at high temperatures, it is essential to know the degradation temperatures for a better process design [4, 226].

The presence of reinforcing agents in the matrix can increase the thermal stability in different ways. First, they can act as a barrier, which makes them useful for flame retardation applications [209, 227, 228]. Second,

they can create a network which can protect the polymer from degradation [229–232]. Third, they can act as radical traps [233]; and lastly, they are capable of altering the microstructure of the product [4, 222]. Moreover, strong adhesion between the filler and matrix causes lower mobility of polymer chains followed by reduction of decomposition rate [234, 235]. Therefore, using any method which can increase the strength of the interaction between the composite constituents would improve its thermal stability.

5.3 Thermal conductivity

In many literatures, it has been confirmed that the interface in the composites play a significant role in their thermal

Fig. 13 Proposed microstructure evolution in polymer-filler [280]

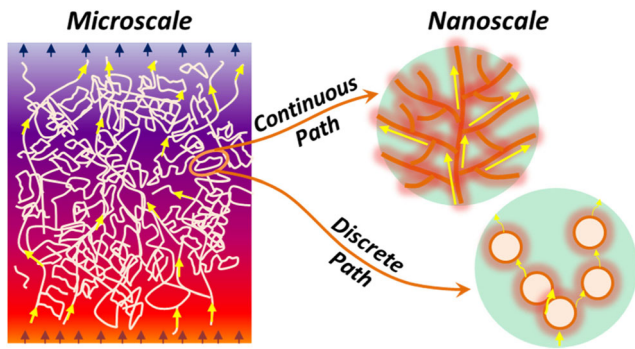


Fig. 14 Schematic illustration of different crystalline structure and subsequent micro- and nanoscale phonon transfer in different PVA-AA blends [290]

conductivity [236–241]. Heat transfer at the interface of two different materials mostly happens with a temperature discontinuity [242]. This phenomenon was observed first at the interface of a metal and liquid helium [243], while later it has been found at the interface of two solids [244]. The heat loss at the interface of two different materials is due to the phonon scattering at this region [236, 238, 239]. Phonon scattering can be significantly impacted by dimensions of fillers, the matrix, and their interfacial regions. Therefore, the interfacial zones predominantly affect the thermal conductivity of the composite [245, 246]. As a result, anything that can affect the interfacial regions (e.g., geometry of particles [247–253], aggregation [254–256], interfacial pressure [257], roughness [258–260], and the strength of

interactions at the interfaces [261–265]) in the composites would influence their thermal conductivity. In this section, we will review the parameters affecting the interfacial interactions and their subsequent impact on the thermal conductivity of the composites.

The heat transport in the macroscopic scale can be described by the Fourier law ($k = Q/\Delta T$), where k is the thermal conduction coefficients and it relates the heat flux (Q) to the temperature gradient. The thermal conductivity at the boundaries is explained by the following equation, $h_{BD} = Q_1/\Delta T_1$, where h_{BD} is the thermal boundary conductance, Q_1 is the heat flux perpendicular to the interface, and ΔT_1 is the temperature discontinuity. The thermal boundary conductance, which is the inverse of the interfacial thermal resistance, was studied first by Kapitza in 1941 [243]. The effects of interfacial phonons transport are merged into this factor [238]. Although in macroscopic scale k is the controlling parameter for heat flux, it is strongly affected by h_{BD} at nanoscale [266, 267]. In this regard, interface plays a key role because of influence of factors such as lattice mismatch [256, 268] and phonon scattering [267, 269]. Wang et al. reported that the interfacial resistance and phonon scattering are due to the incomplete contact at the interface (MWCNTs in their study) [270]. Moreover, it has been reported that the resistance of the solid-liquid interface is a function of properties of adsorbed liquid layers [271]. Presence of adsorbed polymer layers around the fillers prevent the formation of percolation network and filler-filler phonon transfer. Even if the fillers are in direct contact with each other, due to their

Fig. 15 Schematic drawing of intermolecular interactions in PVA-lignin-gelatin blend via H-bonding and achieved continuous coil microstructures [292]

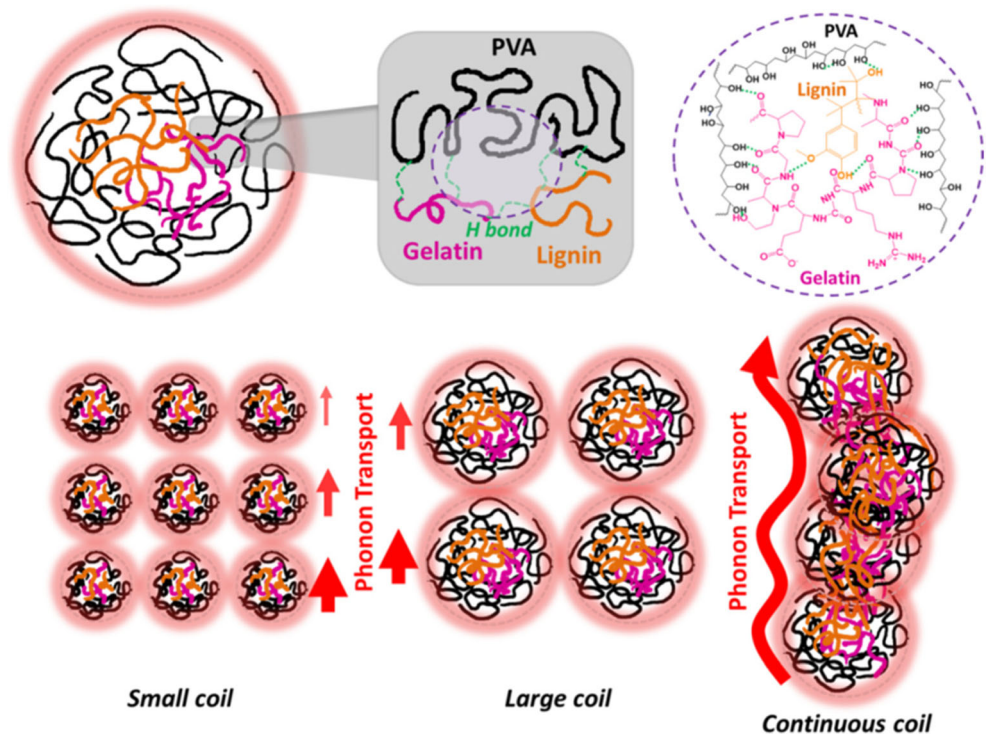


Table 3 Effect of filler type and surface functionalization on thermal conductivity of polymer composites

Filler	Fraction	Matrix	TC change	Ref.
MWCNTs@SiO ₂ -g-BMI ^a	1.25 wt%	Epoxy	+ 125%	[295]
Noncovalent functionalization with pyrene carboxylic acid, BNNTs ^b -BNNSs ^c (BN) ^d -coated polymethylsilsesquioxane	1 vol%	Epoxy	+ 95%	[296]
Noncovalent functionalized graphene nanosheets	30 vol%	Epoxy	+ 9 times	[297]
Silica-coated aluminum nitride	1 phr	Epoxy	+ 267%	[275]
	50 vol%	Epoxy	+ 10 times	[298]
GA-II ^e anchored graphene (noncovalent)	2 wt%	Epoxy	+ 12 times	[171]
Noncovalent functionalized graphene flakes	10 wt%	Epoxy	+ 665%	[216]
GNP-C750	5 wt%	Epoxy	+ 115%	[178]
Alumina-coated graphene sheet	40 wt%	PVDF	+ 192%	[299]
Alumina-decorated graphene nanoplatelets	12 wt%	Epoxy	+ 677%	[300]
Functionalized GNPs	29.3 vol%	Polyphenylene sulfide (PPS)	+ 19 times	[301]
SiC _{NWS} ^f -graphene sheets	7 wt%	PI	+ 138%	[302]
Graphene-graphene oxide	10 wt%	Polyamide-6	+ 6 times	[303]
ApPOSS-graphene ^g	0.25 wt%	Epoxy	+ 37.60%	[304]
	0.5 wt%		+ 57.90%	
Noncovalently modified graphene nanosheets		PU	+ 34%	[305]
	0.608 - wt%			
TCA-rGO ^h	5 wt%	Polyamide	+ 19 times	[306]

^a 1,10-(Methylene di-4,1-phenylene) bismaleimide (BMI) was grafted to core-shell MWCNT@SiO₂-NH₂

^b Boron nitride nanotubes

^c Boron nitride nanosheets

^d Boron nitride

^e Bio-based epoxy monomer (GA-II) synthesized from renewable gallic acid

^f One dimensional silicon carbide nanowires

^g Aminopropylisobutyl polyhedral oligomeric silsesquioxane covalently grafted graphene

^h Modified reduced graphene (rGO) with titanate coupling agent

small contact area, the matrix and its interfacial resistance play a key role in heat transfer [272].

Noncovalent functionalization has been used for dispersion of fillers (i.e., CNTs [273, 274] and graphene [171, 275]) in polymer matrix. This type of functionalization enhances the dispersion quality of fillers. However, its impact on the thermal conductivity is still not clear. In some studies, it was observed that contrary to the dispersion of fillers, the thermal conductivity was decreased compared to the untreated fillers [251]. The authors believed that the noncovalent functionalization leads to the formation of more filler-matrix interfaces and higher phonon scattering. Additionally, it was proposed that this type of bonding at the interface cannot effectively transfer the thermal vibration from the filler to the matrix [251]. Contrary to these studies, some other authors showed thermal conductivity improvements with employing the noncovalent functionalization [171, 275, 276]. For example, Teng et al. functionalized graphene nanosheets (GNSs)

through π - π stacking with functionalized pyrene molecules containing functional segmented polymer chains poly(glycidyl methacrylate) (PGMA), Py-PGMA. They showed that Py-PGMA-GNS fillers could form covalent bonding with epoxy. The strong interaction between Py-PGMA-GNS fillers and matrix resulted in a much higher thermal conductivity comparing to composites filled with pristine GNS and MWCNT. Optimized Py-PGMA-GNS-epoxy composite showed 20 and 267% higher thermal conductivity than pristine GNS-epoxy and pristine MWCNT-epoxy, respectively [275].

In the presence of strong bonding, the phonon scattering and the local thermal resistance could be decreased and subsequently improved the thermal conductivity of the composite [277–279]. This phenomenon was explained by increasing the transmission coefficient of the phonons [263, 278]. Modification of the end groups of the polymer chains [261] and surface modification of the fillers (either with

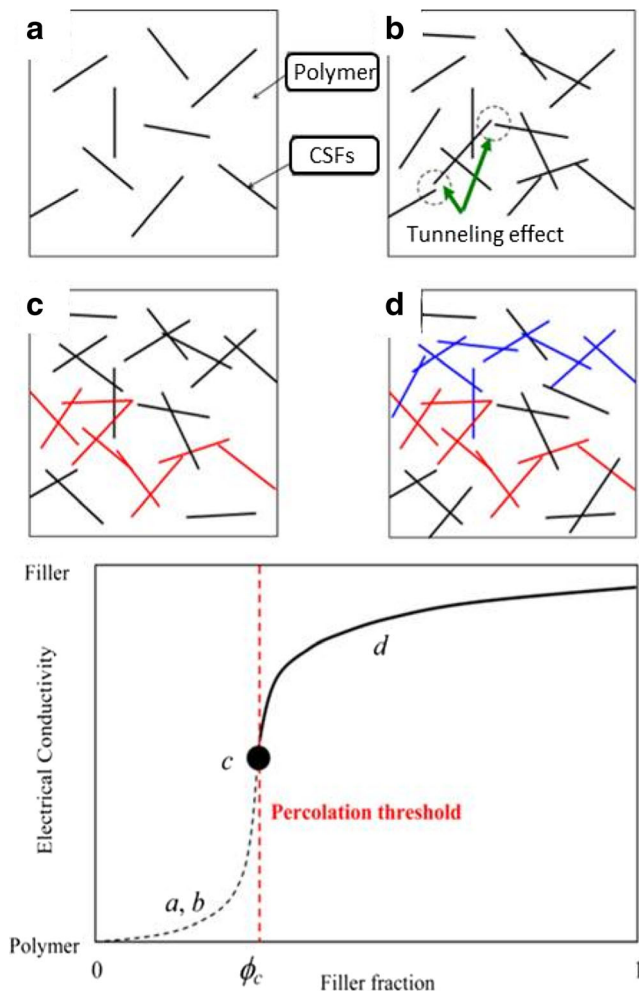


Fig. 16 a–d Percolation stages in conductive composite and the corresponding electrical conductivity in each step [316]

functionalization [237, 280–284] or applying specific coatings [285–287]) are common methods for improving the adhesion at the interfaces with subsequent thermal conductivity enhancement. However, it should be considered that the

functionalization of the filler may create defects and decrease the intrinsic thermal conductivity of them [288]. This is caused by higher phonon scattering at the grafted area. On the other hand, the phonon scattering at the interface will be decreased due to higher compatibility of fillers and matrix after functionalization. Therefore, the reduction of intrinsic thermal conductivity of fillers due to their modification and increment of interfacial thermal conductance at the interface are competing parameters [251].

Huang et al. proposed that there is a critical concentration for thermal conductivity enhancement by chemical bonding. Below this concentration, covalent bonding improved the thermal conductivity; above this concentration, chemical bonding became not as much effective. Although increasing the filler loading could enhance the thermal conductivity through direct contact of the fillers, formation of voids and defects at higher filler concentration could suppress the thermal conductivity enhancement as well (Fig. 13) [280].

In addition to the introduction of conductive fillers in polymeric matrix, the thermal conductivity can be enhanced by engineering the inter-chain interactions [289]. This approach is accompanied with introduction of large crystallinity [290, 291] or hydrogen bonding [289, 292–294] in polymer blends.

Mu et al. studied the effect of incorporation of different types of amino acids (AAs) in poly(vinyl alcohol) (PVA). They showed that depending on the type of PVA-AA interaction, two crystal patterns were formed, continuous and discrete, as shown in Fig. 14. They emphasized the important role of interface surrounding the crystalline pattern. The continuous crystal network created continuous interface with facilitated phonon transfer while the phonon scattering was higher in discrete network. They concluded that high PVA-AA interaction and self-organized continuous crystal structure resulted in higher thermal conductivity in the composite [290].

In another study, the effect of induced H-bonding in PVA-biopolymers (i.e., lignin and gelatin) blend and its subsequent

Table 4 Effect of filler functionalization on electrical conductivity of polymer composites

Filler	Fraction	Matrix	Matrix σ (S/m)	Composite σ (S/m)	Ref.
Poly(phenyleneethynylene) (PPE)-functionalized SWCNT	7 wt%	PS PC	10^{-14} 10^{-13}	6.89 4.81×10^2	[330]
MWCNT	~3 wt%	Polypyrrole	2.42×10^{-2}	0.38	[331]
Trifluorophenyl-functionalized MWCNT	~1.8 wt%	PVDF	$\sim 10^{-8}$	$\sim 10^{-2}$	[332]
Nitric acid-treated MWNT	<1.5 wt%	Waterborne PU	2.5×10^{-12}	1.2×10^{-4}	[333]
Acyl chloride-functionalized MWCNT	0.1 wt%	Nylon 610	2.1×10^{-17}	6.1×10^{-12}	[334]
SWCNT	50 wt%	Polythiophene	1.67×10^{-6}	0.41	[335]
MWCNT	<8 wt%	Poly(3-hexylthiophene) (P3HT)	2.85×10^{-5}	3.56×10^{-3}	[336]
MWCNT	24.8 wt%	Polyaniline	1.1×10^{-2}	1.27	[337]
PPE-functionalized CNT	2 wt%	Poly(benzoyl-1,4-phenylene)-co-(1,3-phenylene)	$< 10^{-11}$	28.6	[338]
Pristine MWCNTs with P3HT-g-polycaprolactone	5 wt%	PC	10^{-15}	6.4×10^{-1}	[339]

impact on thermal conductivity was investigated by Mu et al. They found that stronger H-bonding caused larger polymer coils which created a continuous microstructure. As a result, these formed continuous microstructures of polymer coils led to continuous pathways for better phonon transfer (Fig. 15) [292].

The advantageous of nanofiller incorporation in some other polymeric composites has been summarized in Table 3. In summary, incorporation of thermally conductive fillers, reduction of phonon scattering at the interfacial regions, and enhancement of phonon transfer by enhancing the inter-chain interaction can improve the TC of polymeric materials.

6 Influence of interfacial interactions on electrical conductivity

Contrary to the thermal and mechanical properties of the composites, where homogenous distribution and strong adhesion between the fillers and the matrix is required, electrical conductivity (EC) is based on formation of continuous electrical conductive network between the fillers [307–312]. The electrical conductivity enhancement appears in three main stages, (i) prior to, (ii) within, and (iii) after percolation threshold [313–315]. Figure 16 [316] shows the three steps for carbon fibers into a polymer host, respectively. In the first stage, due to presence of few CFs, EC is close to the EC of the host. Gradually by aggregation and connection through CFs, the EC increases slightly by tunneling effect (Fig. 16b). However, there is no complete pathway for conduction yet. Further increasing the amount of fillers, creates the first conductive pathway (red lines in state c). The volume fraction of fillers at this stage is known as percolation threshold. Adding more filler into the host creates more conductive pathways, which results in the formation of a more conductive network (Fig. 16d). The percolation threshold is determined by a sharp drop of electrical resistance and it depends on the size and shape (aspect ratio) of fillers [308, 317–319], their dispersion [317, 320, 321], interfacial interactions, and alignment [322–324].

The presence of thin layer of polymer matrix around the fillers prevents the formation of continuous network and cause a tunneling barrier between them [325, 326]. Hence, the functionalization of the fillers has two different effects. As it was mentioned earlier, they will enhance the distribution of the fillers into the host [234, 307, 317, 327]. Well-dispersed fillers result in the formation of continuous conductive pathways which in turn enhance electrical conductivity [308, 320, 328]. On the other hand, the interaction of the host with functionalized filler forms an insulating layer on filler's surface [307, 329], which is detrimental for EC enhancement. In general, it has been reported that the negative influence of functionalization was outweighed by its positive effect on

dispersion of fillers [310, 326]. Some other related literatures are summarized in Table 4.

7 Summary and outlook

In this review, an overview of the interfacial region and its important role in overall properties of the composites and especially polymer nanocomposites were provided. Different types of interactions at the interface and the common techniques for their enhancement were introduced. Additionally, it was described how the properties of fillers, such as their aspect ratio and chemistry will impact the interfacial interaction. Moreover, the techniques used for measuring the adhesion between nanotube fillers and polymer matrixes were described. Finally, the influence of interfacial interactions on the mechanical, thermal, and electrical properties of composites was reviewed. In general, the strength of interfacial bonding plays a key role in the properties of composite. For mechanical properties, it influences the load transfer at the boundary. While for thermal properties, it affects the T_g of polymer host, its degradation rate, and thermal conduction across the interface. Lastly, due to the impact of interfacial bonding on the dispersion of fillers in the matrix, it will subsequently affect formation of percolated network and electrical conductivity.

Numerous studies on the polymer composites and their properties show the importance of the polymer-filler interfaces in these types of materials. It has been confirmed that their performance (mechanical, thermal, electrical, etc.) relies significantly on the quality of the interfacial interactions. Therefore, in-depth studies on the impact of interfacial interactions on each property of polymer composites are required. Insight of these fundamental understandings followed by employing suitable methods for achieving optimum interfacial interactions would lead to enhanced performance of polymer composites.

Acknowledgements Acknowledgement is made to the donors of the American Chemical Society Petroleum Research Fund (#55570-DNI10) and NSF (CBET-1603264).

Compliance with ethical standards

Conflict of interest statement The authors declare that they have no conflict of interest.

References

1. Henry A (2013) Thermal transport in polymers. *Annu Rev Heat Transfer* 17:485–520
2. Alexandre M, Dubois P (2000) Polymer-layered silicate nanocomposites: preparation, properties and uses of a new class of materials. *Mater Sci Eng R* 28(1):1–63

3. Zhu J, Wilkie CA (2000) Thermal and fire studies on polystyrene–clay nanocomposites. *Polym Int* 49(10):1158–1163
4. Gilman JW (1999) Flammability and thermal stability studies of polymer layered-silicate (clay) nanocomposites. *Appl Clay Sci* 15(1):31–49
5. Heinrich G, Klüppel M, Vilgis TA (2002) Reinforcement of elastomers. *Curr Opin Solid State Mater Sci* 6(3):195–203
6. Huang H, Liu C, Wu Y, Fan S (2005) Aligned carbon nanotube composite films for thermal management. *Adv Mater* 17(13):1652–1656
7. Biercuk M, Llaguno MC, Radosavljevic M, Hyun J, Johnson AT, Fischer JE (2002) Carbon nanotube composites for thermal management. *Appl Phys Lett* 80(15):2767–2769
8. Choi E, Brooks J, Eaton D, Al-Haik M, Hussaini M, Garmestani H, Li D, Dahmen K (2003) Enhancement of thermal and electrical properties of carbon nanotube polymer composites by magnetic field processing. *J Appl Phys* 94(9):6034–6039
9. Diani J, Fayolle B, Gilormini P (2009) A review on the Mullins effect. *Eur Polym J* 45(3):601–612
10. Mai Y-W, Yu Z-Z (2006) *Polymer nanocomposites*. Woodhead Publishing, Cambridge
11. Kropka JM, Putz KW, Pryamitsyn V, Ganesan V, Green PF (2007) Origin of dynamical properties in PMMA–C60 nanocomposites. *Macromolecules* 40(15):5424–5432
12. Sichel EK (1982) *Carbon black-polymer composites: the physics of electrically conducting composites*. Marcel Dekker Inc, New York
13. Hamed GR (2000) Reinforcement of rubber. *Rubber Chem Technol* 73(3):524–533
14. Adhikari B, Ghosh AK, Maiti S (2000) Developments in carbon black for rubber reinforcement. *J Polym Mater* 17(2):101–125
15. Hamed G (2007) Rubber reinforcement and its classification. *Rubber Chem Technol* 80(3):533–544
16. Rahmat M, Hubert P (2011) Carbon nanotube–polymer interactions in nanocomposites: a review. *Compos Sci Technol* 72(1):72–84
17. Tang LG, Kardos JL (1997) A review of methods for improving the interfacial adhesion between carbon fiber and polymer matrix. *Polym Compos* 18(1):100–113
18. Chen L, Zheng K, Tian X, Hu K, Wang R, Liu C, Li Y, Cui P (2009) Double glass transitions and interfacial immobilized layer in in-situ-synthesized poly (vinyl alcohol)/silica nanocomposites. *Macromolecules* 43(2):1076–1082
19. Chen M, Qu H, Zhu J, Luo Z, Khasanov A, Kucknoor AS, Haldolaarachchige N, Young DP, Wei S, Guo Z (2012) Magnetic electrospun fluorescent polyvinylpyrrolidone nanocomposite fibers. *Polymer* 53(20):4501–4511
20. Robertson CG, Roland C (2008) Glass transition and interfacial segmental dynamics in polymer-particle composites. *Rubber Chem Technol* 81(3):506–522
21. Jouault N, Vallat P, Dalmas F, Said S, Jestin J, Boué F (2009) Well-dispersed fractal aggregates as filler in polymer–silica nanocomposites: long-range effects in rheology. *Macromolecules* 42(6):2031–2040
22. Rittigstein P, Priestley RD, Broadbelt LJ, Torkelson JM (2007) Model polymer nanocomposites provide an understanding of confinement effects in real nanocomposites. *Nat Mater* 6(4):278–282
23. Qian D (2003) Load transfer mechanism in carbon nanotube ropes. *Compos Sci Technol* 63(11):1561–1569
24. Yu M-F, Yakobson BI, Ruoff RS (2000) Controlled sliding and pullout of nested shells in individual multiwalled carbon nanotubes. *J Phys Chem B* 104(37):8764–8767
25. Qian D, Dickey EC, Andrews R, Rantell T (2000) Load transfer and deformation mechanisms in carbon nanotube-polystyrene composites. *Appl Phys Lett* 76(20):2868–2870
26. Jang BZ (1994) *Advanced polymer composites: principles and applications*. ASM International, Materials Park, OH 44073-0002, USA, 1994 305
27. Thostenson ET, Chou T-W (2002) Aligned multi-walled carbon nanotube-reinforced composites: processing and mechanical characterization. *J Phys D Appl Phys* 35(16):L77
28. Crosby AJ, Lee JY (2007) Polymer nanocomposites: the “nano” effect on mechanical properties. *Polym Rev* 47(2):217–229
29. Cadek M, Coleman J, Ryan K, Nicolosi V, Bister G, Fonseca A, Nagy J, Szostak K, Beguin F, Blau W (2004) Reinforcement of polymers with carbon nanotubes: the role of nanotube surface area. *Nano Lett* 4(2):353–356
30. Yang X, Tu Y, Li L, Shang S, X-m T (2010) Well-dispersed chitosan/graphene oxide nanocomposites. *ACS Appl Mater Interfaces* 2(6):1707–1713
31. Tsutsumi N, Takeuchi N, Kiyotsukuri T (1991) Measurement of thermal diffusivity of filler-polyimide composites by flash radiometry. *J. Polym. Sci., Part B: Polym Phys.* 29(9):1085–1093
32. Wu H, Drzal LT (2013) High thermally conductive graphite nanoplatelet/polyetherimide composite by pre-coating: effect of percolation and particle size. *Polym Compos* 34(12):2148–2153
33. Zhou W, Qi S, Tu C, Zhao H, Wang C, Kou J (2007) Effect of the particle size of Al₂O₃ on the properties of filled heat-conductive silicone rubber. *J Appl Polym Sci* 104(2):1312–1318
34. Li T-L, Hsu S-L-C (2010) Enhanced thermal conductivity of polyimide films via a hybrid of micro- and nano-sized boron nitride. *J Phys Chem B* 114(20):6825–6829
35. Kemaloglu S, Ozkoc G, Aytac A (2010) Thermally conductive boron nitride/SEBS/EVA ternary composites: “processing and characterization”. *Polym Compos* 31(8):1398–1408
36. Fu J, Shi L, Zhang D, Zhong Q, Chen Y (2010) Effect of nanoparticles on the performance of thermally conductive epoxy adhesives. *Polym Eng Sci* 50(9):1809–1819
37. Pashayi K, Fard HR, Lai F, Iruvanti S, Plawsky J, Borca-Tasciuc T (2012) High thermal conductivity epoxy-silver composites based on self-constructed nanostructured metallic networks. *J Appl Phys* 111(10):104310
38. Chen H, Ginzburg VV, Yang J, Yang Y, Liu W, Huang Y, Du L, Chen B (2016) Thermal conductivity of polymer-based composites: fundamentals and applications. *Prog Polym Sci* 59:41–85
39. Radford K (1971) The mechanical properties of an epoxy resin with a second phase dispersion. *J Mater Sci* 6(10):1286–1291
40. Spanoudakis J, Young R (1984) Crack propagation in a glass particle-filled epoxy resin. *J Mater Sci* 19(2):473–486
41. Ji XL, Jing JK, Jiang W, Jiang BZ (2002) Tensile modulus of polymer nanocomposites. *Polym Eng Sci* 42(5):983–993
42. Mishra S, Sonawane S, Singh R (2005) Studies on characterization of nano CaCO₃ prepared by the in situ deposition technique and its application in PP-nano CaCO₃ composites. *J Polym Sci Part B Polym Phys* 43(1):107–113
43. Douce J, Boilot J-P, Bateau J, Scodellaro L, Jimenez A (2004) Effect of filler size and surface condition of nano-sized silica particles in polysiloxane coatings. *Thin Solid Films* 466(1):114–122
44. Fu S-Y, Feng X-Q, Lauke B, Mai Y-W (2008) Effects of particle size, particle/matrix interface adhesion and particle loading on mechanical properties of particulate–polymer composites. *Composites Part B* 39(6):933–961
45. Liao K, Li S (2001) Interfacial characteristics of a carbon nanotube–polystyrene composite system. *Appl Phys Lett* 79(25):4225–4227
46. Suhr J, Koratkar N, Keblinski P, Ajayan P (2005) Viscoelasticity in carbon nanotube composites. *Nat Mater* 4(2):134–137
47. Du M, Guo B, Lei Y, Liu M, Jia D (2008) Carboxylated butadiene–styrene rubber/halloysite nanotube nanocomposites: interfacial interaction and performance. *Polymer* 49(22):4871–4876

48. Lordi V, Yao N (2000) Molecular mechanics of binding in carbon-nanotube–polymer composites. *J Mater Res* 15(12):2770–2779
49. Liu W, Wang Y, Wang P, Li Y, Jiang Q, Hu X, Wei Y, Qiu Y, Shahabadi SIS, Lu X (2017) A biomimetic approach to improve the dispersibility, interfacial interactions and toughening effects of carbon nanofibers in epoxy composites. *Composites Part B* 113: 197–205
50. Mu M, Winey KI (2007) Improved load transfer in nanotube/polymer composites with increased polymer molecular weight. *J Phys Chem C* 111(48):17923–17927
51. Gao J, Loi MA, de Carvalho EJJ, dos Santos MC (2011) Selective wrapping and supramolecular structures of polyfluorene–carbon nanotube hybrids. *ACS Nano* 5(5):3993–3999
52. Nish A, Hwang J-Y, Doig J, Nicholas RJ (2007) Highly selective dispersion of single-walled carbon nanotubes using aromatic polymers. *Nat Nanotechnol* 2(10):640–646
53. Hersam MC (2008) Progress towards monodisperse single-walled carbon nanotubes. *Nat Nanotechnol* 3(7):387–394
54. Hirsch A (2002) Functionalization of single-walled carbon nanotubes. *Angew Chem Int Ed* 41(11):1853–1859
55. McCarthy B, Coleman J, Czerw R, Dalton A, In Het Panhuis M, Maiti A, Drury A, Bernier P, Nagy J, Lahr B (2002) A microscopic and spectroscopic study of interactions between carbon nanotubes and a conjugated polymer. *J Phys Chem B* 106(9):2210–2216
56. Zheng M, Jagota A, Semke ED, Diner BA, Mclean RS, Lustig SR, Richardson RE, Tassi NG (2003) DNA-assisted dispersion and separation of carbon nanotubes. *Nat Mater* 2(5):338–342
57. Tallury SS, Pasquini MA (2010) Molecular dynamics simulations of polymers with stiff backbones interacting with single-walled carbon nanotubes. *J Phys Chem B* 114(29):9349–9355
58. Sánchez-Pomales G, Pagán-Miranda C, Santiago-Rodríguez L, Cabrera CR (2010) DNA-wrapped carbon nanotubes: from synthesis to applications. *Carbon nanotubes*. InTech Education and Publishing, Vukovar, 721–748
59. Zheng M, Jagota A, Strano MS, Santos AP, Barone P, Chou SG, Diner BA, Dresselhaus MS, Mclean RS, Onoa GB (2003) Structure-based carbon nanotube sorting by sequence-dependent DNA assembly. *Science* 302(5650):1545–1548
60. Kusner I, Srebnik S (2006) Conformational behavior of semiflexible polymers confined to a cylindrical surface. *Chem Phys Lett* 430(1):84–88
61. Xie Y, Soh A (2005) Investigation of non-covalent association of single-walled carbon nanotube with amylose by molecular dynamics simulation. *Mater Lett* 59(8):971–975
62. Gao H, Kong Y (2004) Simulation of DNA-nanotube interactions. *Annu Rev Mater Res* 34:123–150
63. Ma Y, Ali SR, Doodoo AS, He H (2006) Enhanced sensitivity for biosensors: multiple functions of DNA-wrapped single-walled carbon nanotubes in self-doped polyaniline nanocomposites. *J Phys Chem B* 110(33):16359–16365
64. Ning N, Fu S, Zhang W, Chen F, Wang K, Deng H, Zhang Q, Fu Q (2012) Realizing the enhancement of interfacial interaction in semicrystalline polymer/filler composites via interfacial crystallization. *Prog Polym Sci* 37(10):1425–1455
65. Shaffer MS, Fan X, Windle A (1998) Dispersion and packing of carbon nanotubes. *Carbon* 36(11):1603–1612
66. Hamon MA, Chen J, Hu H, Chen Y, Itkis ME, Rao AM, Eklund PC, Haddon RC (1999) Dissolution of single-walled carbon nanotubes. *Adv Mater* 11(10):834–840
67. Bahr JL, Tour JM (2002) Covalent chemistry of single-wall carbon nanotubes. *J Mater Chem* 12(7):1952–1958
68. Zhu J, Kim J, Peng H, Margrave JL, Khabashesku VN, Barrera EV (2003) Improving the dispersion and integration of single-walled carbon nanotubes in epoxy composites through functionalization. *Nano Lett* 3(8):1107–1113
69. Georgakilas V, Kordatos K, Prato M, Guldi DM, Holzinger M, Hirsch A (2002) Organic functionalization of carbon nanotubes. *JACS* 124(5):760–761
70. Eitan A, Jiang K, Dukes D, Andrews R, Schadler LS (2003) Surface modification of multiwalled carbon nanotubes: toward the tailoring of the interface in polymer composites. *Chem Mater* 15(16):3198–3201
71. Ramanathan T, Abdala A, Stankovich S, Dikin D, Herrera-Alonso M, Piner R, Adamson D, Schniepp H, Chen X, Ruoff R (2008) Functionalized graphene sheets for polymer nanocomposites. *Nat Nanotechnol* 3(6):327–331
72. Varol HS, Sánchez MA, Lu H, Baio JE, Malm C, Encinas N, Mermet-Guyennet MR, Martzel N, Bonn D, Bonn M (2015) Multiscale effects of interfacial polymer confinement in silica nanocomposites. *Macromolecules* 48(21):7929–7937
73. Roy N, Sengupta R, Bhowmick AK (2012) Modifications of carbon for polymer composites and nanocomposites. *Prog Polym Sci* 37(6):781–819
74. Velasco-Santos C, Martínez-Hernández AL, Fisher FT, Ruoff R, Castaño VM (2003) Improvement of thermal and mechanical properties of carbon nanotube composites through chemical functionalization. *Chem Mater* 15(23):4470–4475
75. Koval'chuk AA, Shevchenko VG, Shchegolikhin AN, Nedorezova PM, Klyamkina AN, Aladyshev AM (2008) Effect of carbon nanotube functionalization on the structural and mechanical properties of polypropylene/MWCNT composites. *Macromolecules* 41(20):7536–7542
76. Wang X, Kalali EN, Wang D-Y (2015) An in situ polymerization approach for functionalized MoS₂/nylon-6 nanocomposites with enhanced mechanical properties and thermal stability. *J Mater Chem A* 3(47):24112–24120
77. Zhu J, Peng H, Rodríguez-Macias F, Margrave JL, Khabashesku VN, Inam AM, Lozano K, Barrera EV (2004) Reinforcing epoxy polymer composites through covalent integration of functionalized nanotubes. *Adv Funct Mater* 14(7):643–648
78. Moniruzzaman M, Du F, Romero N, Winey KI (2006) Increased flexural modulus and strength in SWNT/epoxy composites by a new fabrication method. *Polymer* 47(1):293–298
79. Salavagione HJ, Martínez G (2011) Importance of covalent linkages in the preparation of effective reduced graphene oxide–poly(vinyl chloride) nanocomposites. *Macromolecules* 44(8):2685–2692
80. Yuan J-M, Fan Z-F, Chen X-H, Chen X-H, Wu Z-J, He L-P (2009) Preparation of polystyrene–multiwalled carbon nanotube composites with individual-dispersed nanotubes and strong interfacial adhesion. *Polymer* 50(14):3285–3291
81. Choi WS, Ryu SH (2010) Enhancement of dispersion of carbon nanotube and physical properties of poly(styrene-co-acrylonitrile)/multiwalled carbon nanotube nanocomposite via surface initiated ATRP. *Appl Polym Sci* 116(5): 2930–2936
82. Yang B-X, Shi J-H, Pramoda K, Goh SH (2008) Enhancement of the mechanical properties of polypropylene using polypropylene-grafted multiwalled carbon nanotubes. *Compos Sci Technol* 68(12):2490–2497
83. Karthikeyan A, Coulombe S, Kietzig A (2017) Wetting behavior of multi-walled carbon nanotube nanofluids. *Nanotechnology* 28(10):105706
84. Nuril S, Liu L, Barber A, Wagner H (2005) Direct measurement of multiwall nanotube surface tension. *Chem Phys Lett* 404(4): 263–266
85. Tran MQ, Cabral JT, Shaffer MS, Bismarck A (2008) Direct measurement of the wetting behavior of individual carbon nanotubes by polymer melts: the key to carbon nanotube–polymer composites. *Nano Lett* 8(9):2744–2750

86. Dujardin E, Ebbesen TW, Krishnan A, Treacy MM (1998) Wetting of single shell carbon nanotubes. *Adv Mater* 10(17):1472–1475
87. Young T (1805) An essay on the cohesion of fluids. *Philos Trans R Soc London* 95:65–87
88. Zisman WA (1964) Relation of the equilibrium contact angle to liquid and solid constitution. *Adv Chem Ser.* 43:1–51
89. Decco O, Zuchuat J, Farkas N (2017) Improvement of Cr-Co-Mo membrane surface used as barrier for bone regeneration through UV photofunctionalization: an in vitro study. *Materials* 10(7):825
90. Yuan Y, Lee TR (2013) Contact angle and wetting properties. In: *Surface science techniques*. Springer, Berlin Heidelberg, 3–34
91. Qian H, Bismarck A, Greenhalgh ES, Shaffer MS (2010) Carbon nanotube grafted silica fibres: characterising the interface at the single fibre level. *Compos Sci Technol* 70(2):393–399
92. Caroll B (1986) Equilibrium conformation of liquid drops on thin cylinders under forces of capillarity. *Langmuir* 12:248–250
93. Neimark AV (1999) Thermodynamic equilibrium and stability of liquid films and droplets on fibers. *J Adhes Sci Technol* 13(10):1137–1154
94. Qian H, Bismarck A, Greenhalgh ES, Shaffer MS (2010) Carbon nanotube grafted carbon fibres: a study of wetting and fibre fragmentation. *Composites Part A* 41(9):1107–1114
95. Hoecker F, Karger-Kocsis J (1996) Surface energetics of carbon fibers and its effects on the mechanical performance of CF/EP composites. *J Appl Polym Sci* 59(1):139–153
96. Ghenaïm A, Elachari A, Louati M, Caze C (2000) Surface energy analysis of polyester fibers modified by graft fluorination. *J Appl Polym Sci* 75(1):10–15
97. Nishijima H, Kamo S, Akita S, Nakayama Y, Hohmura KI, Yoshimura SH, Takeyasu K (1999) Carbon-nanotube tips for scanning probe microscopy: preparation by a controlled process and observation of deoxyribonucleic acid. *Appl Phys Lett* 74(26):4061–4063
98. Barber AH, Cohen SR, Wagner HD (2004) Static and dynamic wetting measurements of single carbon nanotubes. *Phys Rev Lett* 92(18):186103
99. Barber AH, Cohen SR, Wagner HD (2005) External and internal wetting of carbon nanotubes with organic liquids. *Phys. Rev. B* 71(11):115443
100. Hiura H, Ebbesen T, Tanigaki K, Takahashi H (1993) Raman studies of carbon nanotubes. *Chem Phys Lett* 202(6):509–512
101. Martínez-Rubí Y, Guan J, Lin S, Scriver C, Sturgeon RE, Simard B (2007) Rapid and controllable covalent functionalization of single-walled carbon nanotubes at room temperature. *Chem Commun* 48:5146–5148
102. Nii H, Sumiyama Y, Nakagawa H, Kunishige A (2008) Influence of diameter on the Raman spectra of multi-walled carbon nanotubes. *Appl Phys Express* 1(6):064005
103. Hulman M, Pfeiffer R, Kuzmany H (2004) Raman spectroscopy of small-diameter nanotubes. *New J Phys* 6(1):1
104. Lefrant S, Buisson J, Schreiber J, Chauvet O, Baibarac M, Baltog I (2004) Raman studies of carbon nanotubes and polymer nanotube composites. *Mol Cryst Liq Cryst* 415(1):125–132
105. Schadler L, Giannaris S, Ajayan P (1998) Load transfer in carbon nanotube epoxy composites. *Appl Phys Lett* 73(26):3842–3844
106. Rasheed A, Chae HG, Kumar S, Dadmun MD (2006) Polymer nanotube nanocomposites: correlating intermolecular interaction to ultimate properties. *Polymer* 47(13):4734–4741
107. Baibarac M, Baltog I, Lefrant S (2009) Raman spectroscopic evidence for interfacial interactions in poly(bithiophene)/single-walled carbon nanotube composites. *Carbon* 47(5):1389–1398
108. Ashino M, Schwarz A, Behnke T, Wiesendanger R (2004) Atomic-resolution dynamic force microscopy and spectroscopy of a single-walled carbon nanotube: characterization of interatomic van der Waals forces. *Phys Rev Lett* 93(13):136101
109. Bernard C, Marsaudon S, Boisgard R, Aimé J-P (2007) Competition of elastic and adhesive properties of carbon nanotubes anchored to atomic force microscopy tips. *Nanotechnology* 19(3):035709
110. Li X, Chen W, Zhan Q, Dai L, Sowards L, Pender M, Naik RR (2006) Direct measurements of interactions between polypeptides and carbon nanotubes. *Phys Chem B* 110(25):12621
111. Barber AH, Cohen SR, Wagner HD (2003) Measurement of carbon nanotube–polymer interfacial strength. *Appl Phys Lett* 82(23):4140–4142
112. Strus M, Zalamea L, Raman A, Pipes R, Nguyen C, Stach E (2008) Peeling force spectroscopy: exposing the adhesive nanomechanics of one-dimensional nanostructures. *Nano Lett* 8(2):544–550
113. Wang W, Ciselli P, Kuznetsov E, Peijs T, Barber A (2008) Effective reinforcement in carbon nanotube–polymer composites. *Philos Trans R Soc London Ser A* 366(1870):1613–1626
114. Barber AH, Cohen SR, Kenig S, Wagner HD (2004) Interfacial fracture energy measurements for multi-walled carbon nanotubes pulled from a polymer matrix. *Compos Sci Technol* 64(15):2283–2289
115. Barber A, Cohen S, Wagner H (2004) Stepped polymer morphology induced by a carbon nanotube tip. *Nano Lett* 4(8):1439–1443
116. Strus MC, Cano CI, Pipes RB, Nguyen CV, Raman A (2009) Interfacial energy between carbon nanotubes and polymers measured from nanoscale peel tests in the atomic force microscope. *Compos Sci Technol* 69(10):1580–1586
117. Poggi MA, Bottomley LA, Lillehei PT (2004) Measuring the adhesion forces between alkanethiol-modified AFM cantilevers and single walled carbon nanotubes. *Nano Lett* 4(1):61–64
118. Poggi MA, Lillehei PT, Bottomley LA (2005) Chemical force microscopy on single-walled carbon nanotube paper. *Chem Mater* 17(17):4289–4295
119. Friddle RW, Lemieux MC, Cicero G, Artyukhin AB, Tsukruk VV, Grossman JC, Galli G, Noy A (2007) Single functional group interactions with individual carbon nanotubes. *Nat Nanotechnol* 2(11):692–697
120. Rahmat M, Hubert P (2010) Interaction stress measurement using atomic force microscopy: a stepwise discretization method. *J Phys Chem C* 114(35):15029–15035
121. Rahmat M, Das K, Hubert P (2011) Interaction stresses in carbon nanotube-polymer nanocomposites. *ACS Appl Mater Interfaces* 3(9):3425–3431
122. Rahmat M, Ghiasi H, Hubert P (2012) An interaction stress analysis of nanoscale elastic asperity contacts. *Nano* 4(1):157–166
123. Tjong SC (2006) Structural and mechanical properties of polymer nanocomposites. *Mater Sci Eng R* 53(3):73–197
124. Bartzczak Z, Argon A, Cohen R, Weinberg M (1999) Toughness mechanism in semi-crystalline polymer blends: II. High-density polyethylene toughened with calcium carbonate filler particles. *Polymer* 40(9):2347–2365
125. Misra R, Nerikar P, Bertrand K, Murphy D (2004) Some aspects of surface deformation and fracture of 5–20% calcium carbonate-reinforced polyethylene composites. *Mater Sci Eng A* 384(1):284–298
126. Zhu J, Wei S, Alexander MJ, Cocke D, Ho TC, Guo Z (2010) Electrical conductivity manipulation and switching phenomena of poly(p-phenylenebenzobisthiazole) thin film by doping process. *J Mater Chem* 20:568–574
127. Calvert P (1999) Nanotube composites: a recipe for strength. *Nature* 399(6733):210–211
128. Gojny F, Wichmann M, Köpke U, Fiedler B, Schulte K (2004) Carbon nanotube-reinforced epoxy-composites: enhanced stiffness and fracture toughness at low nanotube content. *Compos Sci Technol* 64(15):2363–2371

129. Sahoo NG, Rana S, Cho JW, Li L, Chan SH (2010) Polymer nanocomposites based on functionalized carbon nanotubes. *Prog Polym Sci* 35(7):837–867
130. Ou Y, Yang F, Yu ZZ (1998) A new conception on the toughness of nylon 6/silica nanocomposite prepared via in situ polymerization. *J. Polym. Sci., Part B: Polym Phys* 36(5):789–795
131. Gong T, Liu M-Q, Liu H, Peng S-P, Li T, Bao R-Y, Yang W, Xie B-H, Yang M-B, Guo Z (2017) Selective distribution and migration of carbon nanotubes enhanced electrical and mechanical performances in polyolefin elastomers. *Polymer* 110:1–11
132. Shofner ML, Khabashesku VN, Barrera EV (2006) Processing and mechanical properties of fluorinated single-wall carbon nanotube–polyethylene composites. *Chem Mater* 18(4):906–913
133. Blake R, Coleman JN, Byrne MT, McCarthy JE, Perova TS, Blau WJ, Fonseca A, Nagy JB, Gun'ko YK (2006) Reinforcement of poly (vinyl chloride) and polystyrene using chlorinated polypropylene grafted carbon nanotubes. *J Mater Chem* 16(43):4206–4213
134. Xiao K, Zhang L, Zarudi I (2007) Mechanical and rheological properties of carbon nanotube-reinforced polyethylene composites. *Compos Sci Technol* 67(2):177–182
135. Yang BX, Pramoda KP, Xu GQ, Goh SH (2007) Mechanical reinforcement of polyethylene using polyethylene-grafted multiwalled carbon nanotubes. *Adv Funct Mater* 17(13):2062–2069
136. Lee J-Y, Zhang Q, Emrick T, Crosby AJ (2006) Nanoparticle alignment and repulsion during failure of glassy polymer nanocomposites. *Macromolecules* 39(21):7392–7396
137. Hsiao C-C, Lin TS, Cheng LY, Ma C-CM, Yang AC-M (2005) The nanomechanical properties of polystyrene thin films embedded with surface-grafted multiwalled carbon nanotubes. *Macromolecules* 38(11):4811–4818
138. Stafford CM, Guo S, Harrison C, Chiang MY (2005) Combinatorial and high-throughput measurements of the modulus of thin polymer films. *Rev Sci Instrum* 76(6):062207
139. Stafford CM, Harrison C, Beers KL, Karim A, Amis EJ, VanLandingham MR, Kim H-C, Volksen W, Miller RD, Simonyi EE (2004) A buckling-based metrology for measuring the elastic moduli of polymeric thin films. *Nat Mater* 3(8):545–550
140. Stafford CM, Vogt BD, Harrison C, Julthongpipit D, Huang R (2006) Elastic moduli of ultrathin amorphous polymer films. *Macromolecules* 39(15):5095–5099
141. Dekkers M, Heikens D (1983) The effect of interfacial adhesion on the tensile behavior of polystyrene–glass–bead composites. *J Appl Polym Sci* 28(12):3809–3815
142. Fu S-Y, Lauke B (1998) Characterization of tensile behaviour of hybrid short glass fibre/calcite particle/ABS composites. *Composites Part A* 29(5):575–583
143. Zhu ZK, Yang Y, Yin J, Qi ZN (1999) Preparation and properties of organosoluble polyimide/silica hybrid materials by sol–gel process. *J Appl Polym Sci* 73(14):2977–2984
144. Zhu J, Mu L, Chen L, Shi Y, Wang H, Feng X, Lu X (2014) Interface-strengthened polyimide/carbon nanofibers nanocomposites with superior mechanical and tribological properties. *Macromol Chem Phys* 215(14):1407–1414
145. Q-l X, X-g T (2015) Atomistic modeling of mechanical characteristics of CNT-polyethylene with interfacial covalent interaction. *J Nanomater* 237520:1–9
146. Ramanathan T, Liu H, Brinson L (2005) Functionalized SWNT/polymer nanocomposites for dramatic property improvement. *J. Polym Sci Part B Polym Phys*. 43(17):2269–2279
147. Zhang J, Jia Z, Jia D, Zhang D, Zhang A (2014) Chemical functionalization for improving dispersion and interfacial bonding of halloysite nanotubes in epoxy nanocomposites. *High Perform Polym* 26(7):734–743
148. Thio Y, Argon A, Cohen R (2004) Role of interfacial adhesion strength on toughening polypropylene with rigid particles. *Polymer* 45(10):3139–3147
149. Wu CL, Zhang MQ, Rong MZ, Friedrich K (2005) Silica nanoparticles filled polypropylene: effects of particle surface treatment, matrix ductility and particle species on mechanical performance of the composites. *Compos Sci Technol* 65(3):635–645
150. Frankland S, Caglar A, Brenner D, Griebel M (2002) Molecular simulation of the influence of chemical cross-links on the shear strength of carbon nanotube–polymer interfaces. *J Phys Chem B* 106(12):3046–3048
151. Gao J, Itkis ME, Yu A, Bekyarova E, Zhao B, Haddon RC (2005) Continuous spinning of a single-walled carbon nanotube–nylon composite fiber. *JACS* 127(11):3847–3854
152. An L, Pan Y, Shen X, Lu H, Yang Y (2008) Rod-like attapulgite/polyimide nanocomposites with simultaneously improved strength, toughness, thermal stability and related mechanisms. *J Mater Chem* 18(41):4928–4941
153. Safaei M, Sheidaei A, Baniassadi M, Ahzi S, Mosavi Mashhadi M, Pourboghra F (2015) An interfacial debonding-induced damage model for graphite nanoplatelet polymer composites. *Omput. Mater Sci* 96:191–199
154. Chen M, Lu Z (2015) A comparative study of the load transfer mechanisms of the carbon nanotube reinforced polymer composites with interfacial crystallization. *Composites Part B* 79:114–123
155. Liff SM, Kumar N, McKinley GH (2007) High-performance elastomeric nanocomposites via solvent-exchange processing. *Nat Mater* 6(1):76–83
156. Wang K, Chen L, Wu J, Toh ML, He C, Yee AF (2005) Epoxy nanocomposites with highly exfoliated clay: mechanical properties and fracture mechanisms. *Macromolecules* 38(3):788–800
157. Friedrich K, Fakirov S, Zhang Z (2005) *Polymer composites: from nano- to macro-scale*. Springer Science & Business Media, New York
158. Michler GH, Balta-Calleja FJ (2016) *Mechanical properties of polymers based on nanostructure and morphology*, vol 71. CRC Press, Florida
159. Moloney A, Kausch H, Kaiser T, Beer H (1987) Parameters determining the strength and toughness of particulate filled epoxide resins. *J Mater Sci* 22(2):381–393
160. Ash BJ, Siegel RW, Schadler LS (2004) Mechanical behavior of alumina/poly (methyl methacrylate) nanocomposites. *Macromolecules* 37(4):1358–1369
161. Johnsen B, Kinloch A, Mohammed R, Taylor A, Sprenger S (2007) Toughening mechanisms of nanoparticle-modified epoxy polymers. *Polymer* 48(2):530–541
162. Sakai M, Miyajima T, Inagaki M (1991) Fracture toughness and fiber bridging of carbon fiber reinforced carbon composites. *Compos Sci Technol* 40(3):231–250
163. Boo W, Sun L, Liu J, Clearfield A, Sue H-J, Mullins M, Pham H (2007) Morphology and mechanical behavior of exfoliated epoxy/ α -zirconium phosphate nanocomposites. *Compos Sci Technol* 67(2):262–269
164. Moloney A, Kausch H, Stieger H (1984) The fracture of particulate-filled epoxide resins. *J Mater Sci* 19(4):1125–1130
165. Liu T, Tjui WC, Tong Y, He C, Goh SS, Chung TS (2004) Morphology and fracture behavior of intercalated epoxy/clay nanocomposites. *J Appl Polym Sci* 94(3):1236–1244
166. Zuiderduin W, Huetink J, Gaymans R (2006) Rigid particle toughening of aliphatic polyketone. *Polymer* 47(16):5880–5887
167. Zuiderduin W, Westzaan C, Huetink J, Gaymans R (2003) Toughening of polypropylene with calcium carbonate particles. *Polymer* 44(1):261–275
168. Levita G, Marchetti A, Lazzeri A (1989) Fracture of ultrafine calcium carbonate/polypropylene composites. *Polym Compos* 10(1):39–43

169. Fiedler B, Gojny FH, Wichmann MH, Nolte MC, Schulte K (2006) Fundamental aspects of nano-reinforced composites. *Compos Sci Technol* 66(16):3115–3125
170. Gojny FH, Wichmann MH, Fiedler B, Schulte K (2005) Influence of different carbon nanotubes on the mechanical properties of epoxy matrix composites—a comparative study. *Compos Sci Technol* 65(15):2300–2313
171. Cao L, Liu X, Na H, Wu Y, Zheng W, Zhu J (2013) How a bio-based epoxy monomer enhanced the properties of diglycidyl ether of bisphenol A (DGEBA)/graphene composites. *J Mater Chem A* 1(16):5081–5088
172. Sahoo NG, Cheng HKF, Cai J, Li L, Chan SH, Zhao J, Yu S (2009) Improvement of mechanical and thermal properties of carbon nanotube composites through nanotube functionalization and processing methods. *Mater Chem Phys* 117(1):313–320
173. Chang C-M, Liu Y-L (2010) Functionalization of multi-walled carbon nanotubes with non-reactive polymers through an ozone-mediated process for the preparation of a wide range of high performance polymer/carbon nanotube composites. *Carbon* 48(4):1289–1297
174. Shim HC, Kwak YK, Han C-S, Kim S (2009) Enhancement of adhesion between carbon nanotubes and polymer substrates using microwave irradiation. *Scr Mater* 61(1):32–35
175. Buffa F, Abraham GA, Grady BP, Resasco D (2007) Effect of nanotube functionalization on the properties of single-walled carbon nanotube/polyurethane composites. *J Polym Sci Part B Polym Phys.* 45(4):490–501
176. Blake R, Gun'ko YK, Coleman J, Cadek M, Fonseca A, Nagy JB, Blau WJ (2004) A generic organometallic approach toward ultra-strong carbon nanotube polymer composites. *JACS* 126(33):10226–10227
177. Xie L, Xu F, Qiu F, Lu H, Yang Y (2007) Single-walled carbon nanotubes functionalized with high bonding density of polymer layers and enhanced mechanical properties of composites. *Macromolecules* 40(9):3296–3305
178. Wang F, Drzal LT, Qin Y, Huang Z (2015) Mechanical properties and thermal conductivity of graphene nanoplatelet/epoxy composites. *J Mater Sci* 50(3):1082–1093
179. Wan Y-J, Tang L-C, Gong L-X, Yan D, Li Y-B, Wu L-B, Jiang J-X, Lai G-Q (2014) Grafting of epoxy chains onto graphene oxide for epoxy composites with improved mechanical and thermal properties. *Carbon* 69:467–480
180. Ash BJ, Siegel RW, Schadler LS (2004) Glass-transition temperature behavior of alumina/PMMA nanocomposites. *J Polym Sci Part B Polym Phys.* 42(23):4371–4383
181. Alcoutlabi M, McKenna GB (2005) Effects of confinement on material behaviour at the nanometre size scale. *J Phys Condens Matter* 17(15):R461
182. Napolitano S, Glynos E, Tito NB (2017) Glass transition of polymers in bulk, confined geometries, and near interfaces. *Rep Prog Phys* 80(3):036602
183. Fragiadakis D, Pissis P, Bokobza L (2005) Glass transition and molecular dynamics in poly (dimethylsiloxane)/silica nanocomposites. *Polymer* 46(16):6001–6008
184. Bogoslovov R, Roland C, Ellis A, Randall A, Robertson C, Co A, Leal GL, Colby RH, Giacomini AJ (2008) Effect of silica nanoparticles on the local segmental dynamics in polyvinylacetate. *AIP Conf Proc* 1:1315–1317
185. Legrand A, Lecomte N, Vidal A, Haidar B, Papirer E (1992) Application of NMR spectroscopy to the characterization of elastomer/filler interactions. *J Appl Polym Sci* 46(12):2223–2232
186. Garcia-Fuentes M, Torres D, Martín-Pastor M, Alonso MJ (2004) Application of NMR spectroscopy to the characterization of PEG-stabilized lipid nanoparticles. *Langmuir* 20(20):8839–8845
187. Dybowski C, Vaughan R (1975) Motional phenomena and multiple pulse nuclear magnetic resonance. Nonisotropic motion in natural rubber. *Macromolecules* 8(1):50–54
188. Schaefer J, Chin SH, Weissman S (1972) Magic-angle carbon-13 nuclear magnetic resonance spectra of filled rubber. *Macromolecules* 5(6):798–801
189. Dutta N, Choudhury NR, Haidar B, Vidal A, Donnet J, Delmotte L, Chezeau J (1994) High resolution solid-state NMR investigation of the filler-rubber interaction: 1. High speed ^1H magic-angle spinning NMR spectroscopy in carbon black filled styrene-butadiene rubber. *Polymer* 35(20):4293–4299
190. Litvinov V, Steeman P (1999) EPDM–carbon black interactions and the reinforcement mechanisms, as studied by low-resolution ^1H NMR. *Macromolecules* 32(25):8476–8490
191. Kenny J, McBrierty V, Rigbi Z, Douglass D (1991) Carbon black filled natural rubber. I, structural investigations. *Macromolecules* 24(2):436–443
192. O'brien J, Cashell E, Wardell G, McBrierty V (1976) An NMR investigation of the interaction between carbon black and cis-polybutadiene. *Macromolecules* 9(4):653–660
193. Arrighi V, Higgins J, Burgess A, Floudas G (1998) Local dynamics of poly (dimethyl siloxane) in the presence of reinforcing filler particles. *Polymer* 39(25):6369–6376
194. Nakatani A, Ivkov R, Papanek P, Yang H, Gerspacher M (2000) Inelastic neutron scattering from filled elastomers. *Rubber Chem Technol* 73(5):847–863
195. Tsagaropoulos G, Eisenberg A (1995) Dynamic mechanical study of the factors affecting the two glass transition behavior of filled polymers. Similarities and differences with random ionomers. *Macromolecules* 28(18):6067–6077
196. Tsagaropoulos G, Eisenberg A (1995) Direct observation of two glass transitions in silica-filled polymers. Implications to the morphology of random ionomers. *Macromolecules* 28(1):396–398
197. Berriot J, Montes H, Lequeux F, Long D, Sotta P (2002) Evidence for the shift of the glass transition near the particles in silica-filled elastomers. *Macromolecules* 35(26):9756–9762
198. Gauthier C, Reynaud E, Vassoille R, Ladouce-Stelandre L (2004) Analysis of the non-linear viscoelastic behaviour of silica filled styrene butadiene rubber. *Polymer* 45(8):2761–2771
199. Arrighi V, McEwen I, Qian H, Prieto MS (2003) The glass transition and interfacial layer in styrene-butadiene rubber containing silica nanofiller. *Polymer* 44(20):6259–6266
200. González-Irún Rodríguez J, Carreira P, García-Diez A, Hui D, Artiaga R, Liz-Marzán L (2007) Nanofiller effect on the glass transition of a polyurethane. *J Therm Anal Calorim* 87(1):45–47
201. López-Martínez EI, Márquez-Lucero A, Hernández-Escobar CA, Flores-Gallardo SG, Ibarra-Gómez R, Yacamán MJ, Zaragoza-Contreras EA (2007) Incorporation of silver/carbon nanoparticles into poly (methyl methacrylate) via in situ miniemulsion polymerization and its influence on the glass-transition temperature. *J Polym Sci Part B Polym Phys.* 45(5):511–518
202. Bansal A, Yang H, Li C, Benicewicz BC, Kumar SK, Schadler LS (2006) Controlling the thermomechanical properties of polymer nanocomposites by tailoring the polymer–particle interface. *J Polym Sci Part B Polym Phys.* 44(20):2944–2950
203. Kraus G, Gruver J (1970) Thermal expansion, free volume, and molecular mobility in a carbon black-filled elastomer. *J Polym Sci Part B Polym Phys.* 8(4):571–581
204. Rittigstein P, Torkelson JM (2006) Polymer–nanoparticle interfacial interactions in polymer nanocomposites: Confinement effects on glass transition temperature and suppression of physical aging. *J Polym Sci Part B Polym Phys.* 44(20):2935–2943
205. Ou YC, Yu ZZ, Vidal A, Donnet J (1996) Effects of alkylation of silicas on interfacial interaction and molecular motions between silicas and rubbers. *J Appl Polym Sci* 59(8):1321–1328

206. Tian X, Zhang X, Liu W, Zheng J, Ruan C, Cui P (2006) Preparation and properties of poly (ethylene terephthalate)/silica nanocomposites. *J Macromol Sci Part B Phys* 45(4):507–513
207. Huang X, Brittain WJ (2001) Synthesis and characterization of PMMA nanocomposites by suspension and emulsion polymerization. *Macromolecules* 34(10):3255–3260
208. Mackay ME, Dao TT, Tuteja A, Ho DL, Van Horn B, Kim H-C, Hawker CJ (2003) Nanoscale effects leading to non-Einstein-like decrease in viscosity. *Nat Mater* 2(11):762–766
209. Hu L, Jiang P, Zhang P, Bian G, Sheng S, Huang M, Bao Y, Xia J (2016) Amine-graphene oxide/waterborne polyurethane nanocomposites: effects of different amine modifiers on physical properties. *J Mater Sci* 51(18):8296–8309
210. Chang JH, Mun MK, Kim JC (2007) Synthesis and characterization of poly (butylene terephthalate)/mica nanocomposite fibers via in situ interlayer polymerization. *J Appl Polym Sci* 106(2):1248–1255
211. Xu W, Zhou Z, Ge M, Pan W-P (2004) Polyvinyl chloride/montmorillonite nanocomposites. *J Therm Anal Calorim* 78(1):91–99
212. Huskić M, Žigon M (2007) PMMA/MMT nanocomposites prepared by one-step in situ intercalative solution polymerization. *Eur Polym J* 43(12):4891–4897
213. Shi X, Gan Z (2007) Preparation and characterization of poly (propylene carbonate)/montmorillonite nanocomposites by solution intercalation. *Eur Polym J* 43(12):4852–4858
214. Sun Y, Luo Y, Jia D (2008) Preparation and properties of natural rubber nanocomposites with solid-state organomodified montmorillonite. *J Appl Polym Sci* 107(5):2786–2792
215. Uthirakumar P, Nahm KS, Hahn YB, Lee Y-S (2004) Preparation of polystyrene/montmorillonite nanocomposites using a new radical initiator-montmorillonite hybrid via in situ intercalative polymerization. *Eur Polym J* 40(11):2437–2444
216. Song SH, Park KH, Kim BH, Choi YW, Jun GH, Lee DJ, Kong BS, Paik KW, Jeon S (2013) Enhanced thermal conductivity of epoxy-graphene composites by using non-oxidized graphene flakes with non-covalent functionalization. *Adv Mater* 25(5):732–737
217. Pham JQ, Mitchell CA, Bahr JL, Tour JM, Krishnamoorti R, Green PF (2003) Glass transition of polymer/single-walled carbon nanotube composite films. *J Polym Sci Part B Polym Phys* 41(24):3339–3345
218. Bohning M, Goering H, Hao N, Mach R, Oleszak F, Schonhals A (2003) Molecular mobility and gas transport properties of polycarbonate-based nanocomposites. *Rev Adv Mater Sci* 5(3):155–159
219. Yuen S-M, Ma C-CM, Lin Y-Y, Kuan H-C (2007) Preparation, morphology and properties of acid and amine modified multiwalled carbon nanotube/polyimide composite. *Compos Sci Technol* 67(11):2564–2573
220. He L, Wang H, Xia G, Sun J, Song R (2014) Chitosan/graphene oxide nanocomposite films with enhanced interfacial interaction and their electrochemical applications. *Appl Surf Sci* 314:510–515
221. Hatui G, Bhattacharya P, Sahoo S, Dhivar S, Das CK (2014) Combined effect of expanded graphite and multiwall carbon nanotubes on the thermo mechanical, morphological as well as electrical conductivity of in situ bulk polymerized polystyrene composites. *Composites Part A* 56:181–191
222. Salavagione HJ, Gomez MA, Martínez G (2009) Polymeric modification of graphene through esterification of graphite oxide and poly (vinyl alcohol). *Macromolecules* 42(17):6331–6334
223. Bansal A, Yang H, Li C, Cho K, Benicewicz BC, Kumar SK, Schadler LS (2005) Quantitative equivalence between polymer nanocomposites and thin polymer films. *Nat Mater* 4(9):693–698
224. Pandey JK, Reddy KR, Kumar AP, Singh R (2005) An overview on the degradability of polymer nanocomposites. *Polym Degrad Stab* 88(2):234–250
225. Blumstein A (1965) Polymerization of adsorbed monolayers. II. Thermal degradation of the inserted polymer. *J Polym Sci Part A Polym Chem* 3(7):2665–2672
226. Pieliachowski K, Leszczynska A (2006) Polyoxymethylene-based nanocomposites with montmorillonite: an introductory study. *Polimery* 51(2):143–149
227. Cao Y, Lai Z, Feng J, Wu P (2011) Graphene oxide sheets covalently functionalized with block copolymers via click chemistry as reinforcing fillers. *J Mater Chem* 21(25):9271–9278
228. Park S-J, Seo D-I, Lee J-R (2002) Surface modification of montmorillonite on surface acid–base characteristics of clay and thermal stability of epoxy/clay nanocomposites. *J Colloid Interface Sci* 251(1):160–165
229. Kashiwagi T, Grulke E, Hilding J, Groth K, Harris R, Butler K, Shields J, Kharchenko S, Douglas J (2004) Thermal and flammability properties of polypropylene/carbon nanotube nanocomposites. *Polymer* 45(12):4227–4239
230. Kashiwagi T, Du F, Winey KI, Groth KM, Shields JR, Bellayer SP, Kim H, Douglas JF (2005) Flammability properties of polymer nanocomposites with single-walled carbon nanotubes: effects of nanotube dispersion and concentration. *Polymer* 46(2):471–481
231. Kashiwagi T, Du F, Douglas JF, Winey KI, Harris RH, Shields JR (2005) Nanoparticle networks reduce the flammability of polymer nanocomposites. *Nat Mater* 4(12):928–933
232. Yadav SK, Cho JW (2013) Functionalized graphene nanoplatelets for enhanced mechanical and thermal properties of polyurethane nanocomposites. *Appl Surf Sci* 266:360–367
233. Zhu J, Uhl FM, Morgan AB, Wilkie CA (2001) Studies on the mechanism by which the formation of nanocomposites enhances thermal stability. *Chem Mater* 13(12):4649–4654
234. Liu N, Luo F, Wu H, Liu Y, Zhang C, Chen J (2008) One-step ionic-liquid-assisted electrochemical synthesis of ionic-liquid-functionalized graphene sheets directly from graphite. *Adv Funct Mater* 18(10):1518–1525
235. Kim H, Abdala AA, Macosko CW (2010) Graphene/polymer nanocomposites. *Macromolecules* 43(16):6515–6530
236. Pettersson S, Mahan G (1990) Theory of the thermal boundary resistance between dissimilar lattices. *Phys Rev B* 42(12):7386
237. He H, Fu R, Shen Y, Han Y, Song X (2007) Preparation and properties of Si₃N₄/PS composites used for electronic packaging. *Compos Sci Technol* 67(11):2493–2499
238. Norris PM, Le NQ, Baker CH (2013) Tuning phonon transport: from interfaces to nanostructures. *J Heat Transfer* 135(6):061604
239. Wang Z, Carter JA, Lagutchev A, Koh YK, Seong N-H, Cahill DG, Dlott DD (2007) Ultrafast flash thermal conductance of molecular chains. *Science* 317(5839):787–790
240. Nan C-W, Liu G, Lin Y, Li M (2004) Interface effect on thermal conductivity of carbon nanotube composites. *Appl Phys Lett* 85(16):3549–3551
241. Hall DE, Moreland JC (2001) Fundamentals of rolling resistance. *Rubber Chem Technol* 74(3):525–539
242. Cahill DG, Ford WK, Goodson KE, Mahan GD, Majumdar A, Maris HJ, Merlin R, Phillpot SR (2003) Nanoscale thermal transport. *J Appl Phys* 93(2):793–818
243. Kapitza P (1941) The study of heat transfer in helium II. *Phys Rev* 60(4):354
244. Swartz ET, Pohl RO (1989) Thermal boundary resistance. *Rev Mod Phys* 61(3):605
245. Kochetov R, Korobko A, Andritsch T, Morshuis P, Picken S, Smit J (2011) Modelling of the thermal conductivity in polymer nanocomposites and the impact of the interface between filler and matrix. *J Phys D Appl Phys* 44(39):395401

246. Costescu R, Cahill D, Fabreguette F, Sechrist Z, George S (2004) Ultra-low thermal conductivity in W/Al₂O₃ nanolaminates. *Science* 303(5660):989–990
247. Park JG, Cheng Q, Lu J, Bao J, Li S, Tian Y, Liang Z, Zhang C, Wang B (2012) Thermal conductivity of MWCNT/epoxy composites: the effects of length, alignment and functionalization. *Carbon* 50(6):2083–2090
248. Li J, Ma PC, Chow WS, To CK, Tang BZ, Kim JK (2007) Correlations between percolation threshold, dispersion state, and aspect ratio of carbon nanotubes. *Adv Funct Mater* 17(16):3207–3215
249. Deng F, Zheng Q-S, Wang L-F, Nan C-W (2007) Effects of anisotropy, aspect ratio, and nonstraightness of carbon nanotubes on thermal conductivity of carbon nanotube composites. *Appl Phys Lett* 90(2):021914
250. Veca LM, Meziani MJ, Wang W, Wang X, Lu F, Zhang P, Lin Y, Fee R, Connell JW, Sun YP (2009) Carbon nanosheets for polymeric nanocomposites with high thermal conductivity. *Adv Mater* 21(20):2088–2092
251. Burger N, Laachachi A, Ferriol M, Lutz M, Toniazio V, Ruch D (2016) Review of thermal conductivity in composites: mechanisms, parameters and theory. *Prog Polym Sci* 61:1–28
252. Smith DK, Pantoya ML (2015) Effect of nanofiller shape on effective thermal conductivity of fluoropolymer composites. *Compos Sci Technol* 118:251–256
253. Chen L, Sun Y-Y, Xu H-F, He S-J, Wei G-S, Du X-Z, Lin J (2016) Analytic modeling for the anisotropic thermal conductivity of polymer composites containing aligned hexagonal boron nitride. *Compos Sci Technol* 122:42–49
254. Prasher R, Evans W, Meakin P, Fish J, Phelan P, Keblinski P (2006) Effect of aggregation on thermal conduction in colloidal nanofluids. *Appl Phys Lett* 89(14):143119
255. Tanimoto M, Yamagata T, Miyata K, Ando S (2013) Anisotropic thermal diffusivity of hexagonal boron nitride-filled polyimide films: effects of filler particle size, aggregation, orientation, and polymer chain rigidity. *ACS Appl Mater Interfaces* 5(10):4374–4382
256. Evans W, Prasher R, Fish J, Meakin P, Phelan P, Keblinski P (2008) Effect of aggregation and interfacial thermal resistance on thermal conductivity of nanocomposites and colloidal nanofluids. *Int J Heat Mass Transf* 51(5):1431–1438
257. Hsieh W-P, Lyons AS, Pop E, Keblinski P, Cahill DG (2011) Pressure tuning of the thermal conductance of weak interfaces. *Phys Rev B* 84(18):184107
258. Hopkins PE, Phinney LM, Serrano JR, Beechem TE (2010) Effects of surface roughness and oxide layer on the thermal boundary conductance at aluminum/silicon interfaces. In: 2010 14th International Heat Transfer Conference. American Society of Mechanical Engineers, 313–319
259. Persson B, Volokitin A, Ueba H (2011) Phononic heat transfer across an interface: thermal boundary resistance. *J Phys Condens Matter* 23(4):045009
260. Chu K, W-s L, Dong H (2013) Role of graphene waviness on the thermal conductivity of graphene. *Physical review B composites. Appl Phys A Mater Sci Process* 111(1):221–225
261. Losego MD, Grady ME, Sottos NR, Cahill DG, Braun PV (2012) Effects of chemical bonding on heat transport across interfaces. *Nat Mater* 11(6):502–506
262. Hu L, Zhang L, Hu M, Wang J-S, Li B, Keblinski P (2010) Phonon interference at self-assembled monolayer interfaces: molecular dynamics simulations. *Phys Rev B* 81(23):235427
263. Hu M, Keblinski P, Schelling PK (2009) Kapitza conductance of silicon–amorphous polyethylene interfaces by molecular dynamics simulations. *Phys Rev B* 79(10):104305
264. Hopkins PE, Baraket M, Barnat EV, Beechem TE, Kearney SP, Duda JC, Robinson JT, Walton SG (2012) Manipulating thermal conductance at metal–graphene contacts via chemical functionalization. *Nano Lett* 12(2):590–595
265. O’Brien PJ, Shenogin S, Liu J, Chow PK, Laurencin D, Mutin PH, Yamaguchi M, Keblinski P, Ramanath G (2013) Bonding-induced thermal conductance enhancement at inorganic heterointerfaces using nanomolecular monolayers. *Nat Mater* 12(2):118–122
266. Hung M-T, Choi O, Ju YS, Hahn H (2006) Heat conduction in graphite-nanoplatelet-reinforced polymer nanocomposites. *Appl Phys Lett* 89(2):023117
267. Hopkins PE, Norris PM (2007) Effects of joint vibrational states on thermal boundary conductance. *Nanoscale Microscale Thermophys Eng* 11(3–4):247–257
268. Huxtable ST, Cahill DG, Shenogin S, Xue L, Ozisik R, Barone P, Usrey M, Strano MS, Siddons G, Shim M (2003) Interfacial heat flow in carbon nanotube suspensions. *Nat Mater* 2(11):731–734
269. Zhou Y, Zhang X, Hu M (2016) An excellent candidate for largely reducing interfacial thermal resistance: a nano-confined mass graded interface. *Nano* 8(4):1994–2002
270. Wang Z, Mu H, Liang J, Tang D (2013) Thermal boundary resistance and temperature dependent phonon conduction in CNT array multilayer structure. *Int J Therm Sci* 74:53–62
271. Nakayama T (1985) New channels of energy transfer across a solid-liquid He interface. *J Phys C Solid State Phys* 18(22):L667
272. Shenogina N, Shenogin S, Xue L, Keblinski P (2005) On the lack of thermal percolation in carbon nanotube composites. *Appl Phys Lett* 87(13):133106
273. Chen RJ, Zhang Y, Wang D, Dai H (2001) Noncovalent sidewall functionalization of single-walled carbon nanotubes for protein immobilization. *JACS* 123(16):3838–3839
274. Simmons TJ, Bult J, Hashim DP, Linhardt RJ, Ajayan PM (2009) Noncovalent functionalization as an alternative to oxidative acid treatment of single wall carbon nanotubes with applications for polymer composites. *ACS Nano* 3(4):865–870
275. Teng C-C, Ma C-CM LC-H, Yang S-Y, Lee S-H, Hsiao M-C, Yen M-Y, Chiou K-C, Lee T-M (2011) Thermal conductivity and structure of non-covalent functionalized graphene/epoxy composites. *Carbon* 49(15):5107–5116
276. Yang S-Y, Lin W-N, Huang Y-L, Tien H-W, Wang J-Y, Ma C-CM, Li S-M, Wang Y-S (2011) Synergetic effects of graphene platelets and carbon nanotubes on the mechanical and thermal properties of epoxy composites. *Carbon* 49(3):793–803
277. Kong J, C-y Z, Cheng X (2013) Novel Cu–Cr alloy matrix CNT composites with enhanced thermal conductivity. *Appl Phys A Mater Sci Process* 112(3):631–636
278. Shenogin S, Xue L, Ozisik R, Keblinski P, Cahill DG (2004) Role of thermal boundary resistance on the heat flow in carbon-nanotube composites. *J Appl Phys* 95(12):8136–8144
279. Yang K, Gu M (2009) The effects of triethylenetetramine grafting of multi-walled carbon nanotubes on its dispersion, filler-matrix interfacial interaction and the thermal properties of epoxy nanocomposites. *Polym Eng Sci* 49(11):2158–2167
280. Huang X, Iizuka T, Jiang P, Ohki Y, Tanaka T (2012) Role of interface on the thermal conductivity of highly filled dielectric epoxy/AlN composites. *J Phys Chem C* 116(25):13629–13639
281. Khare KS, Khabaz F, Khare R (2014) Effect of carbon nanotube functionalization on mechanical and thermal properties of cross-linked epoxy–carbon nanotube nanocomposites: role of strengthening the interfacial interactions. *ACS Appl Mater Interfaces* 6(9):6098–6110
282. Shenogin S, Bodapati A, Xue L, Ozisik R, Keblinski P (2004) Effect of chemical functionalization on thermal transport of carbon nanotube composites. *Appl Phys Lett* 85(12):2229–2231
283. W-b Z, Xu X-l, Yang J-h, Huang T, Zhang N, Wang Y, Z-w Z (2015) High thermal conductivity of poly (vinylidene fluoride)/carbon nanotubes nanocomposites achieved by adding polyvinylpyrrolidone. *Compos Sci Technol* 106:1–8

284. Lee H-J, Han S-W, Kwon Y-D, Tan L-S, Baek J-B (2008) Functionalization of multi-walled carbon nanotubes with various 4-substituted benzoic acids in mild polyphosphoric acid/phosphorous pentoxide. *Carbon* 46(14):1850–1859
285. Zhou Y, Wang L, Zhang H, Bai Y, Niu Y, Wang H (2012) Enhanced high thermal conductivity and low permittivity of polyimide based composites by core-shell Ag@ SiO₂ nanoparticle fillers. *Appl Phys Lett* 101(1):012903
286. Huang L, Zhu P, Li G, Lu DD, Sun R, Wong C (2014) Core-shell SiO₂@ RGO hybrids for epoxy composites with low percolation threshold and enhanced thermo-mechanical properties. *J Mater Chem A* 2(43):18246–18255
287. Kim KT, Dao TD, Jeong HM, Anjanapura RV, Aminabhavi TM (2015) Graphene coated with alumina and its utilization as a thermal conductivity enhancer for alumina sphere/thermoplastic polyurethane composite. *Mater Chem Phys* 153:291–300
288. Gulotto R, Castellino M, Jagdale P, Tagliaferro A, Balandin AA (2013) Effects of functionalization on thermal properties of single-wall and multi-wall carbon nanotube-polymer nanocomposites. *ACS Nano* 7(6):5114–5121
289. Kim G-H, Lee D, Shanker A, Shao L, Kwon MS, Gidley D, Kim J, Pipe KP (2015) High thermal conductivity in amorphous polymer blends by engineered interchain interactions. *Nat Mater* 14(3):295
290. Mu L, Li Y, Mehra N, Ji T, Zhu J (2017) Expedited phonon transfer in interfacially constrained polymer chain along self-organized amino acid crystals. *ACS Appl Mater Interfaces* 9(13):12138–12145
291. Mu L, Ji T, Chen L, Mehra N, Shi Y, Zhu J (2016) Paving the thermal highway with self-organized nanocrystals in transparent polymer composites. *ACS Appl Mater Interfaces* 8(42):29080–29087
292. Mu L, He J, Li Y, Ji T, Mehra N, Shi Y, Zhu J (2017) The molecular origin of efficient phonon transfer in modulated polymer blends: effect of hydrogen bonding on polymer coil size and assembled microstructure. *J Phys Chem C* 121(26):14204–14212
293. Mehra N, Mu L, Ji T, Li Y, Zhu J (2017) Moisture driven thermal conduction in polymer and polymer blends. *Compos Sci Technol* 151:115–123
294. Mehra N, Mu L, Zhu J (2017) Developing heat conduction pathways through short polymer chains in a hydrogen bonded polymer system. *Compos Sci Technol* 148:97–105
295. Yu W, Fu J, Chen L, Zong P, Yin J, Shang D, Lu Q, Chen H, Shi L (2016) Enhanced thermal conductive property of epoxy composites by low mass fraction of organic-inorganic multilayer covalently grafted carbon nanotubes. *Compos Sci Technol* 125:90–99
296. Yan H, Tang Y, Su J, Yang X (2014) Enhanced thermal-mechanical properties of polymer composites with hybrid boron nitride nanofillers. *Appl Phys A Mater Sci Process* 114(2):331–337
297. Kim G, Ryu SH, Lee J-T, Seong K-H, Lee JE, Yoon P-J, Kim B-S, Hussain M, Choa Y-H (2013) Enhancement of thermal conductive pathway of boron nitride coated polymethylsilsesquioxane composite. *J Nanosci Nanotechnol* 13(11):7695–7700
298. Wong C, Bollampally RS (1999) Comparative study of thermally conductive fillers for use in liquid encapsulants for electronic packaging. *IEEE Trans Adv Packag* 22(1):54–59
299. Qian R, Yu J, Wu C, Zhai X, Jiang P (2013) Alumina-coated graphene sheet hybrids for electrically insulating polymer composites with high thermal conductivity. *RSC Adv* 3(38):17373–17379
300. Sun R, Yao H, Zhang H-B, Li Y, Mai Y-W, Yu Z-Z (2016) Decoration of defect-free graphene nanoplatelets with alumina for thermally conductive and electrically insulating epoxy composites. *Compos Sci Technol* 137:16–23
301. Gu J, Xie C, Li H, Dang J, Geng W, Zhang Q (2014) Thermal percolation behavior of graphene nanoplatelets/polyphenylene sulfide thermal conductivity composites. *Polym Compos* 35(6):1087–1092
302. Dai W, Yu J, Liu Z, Wang Y, Song Y, Lyu J, Bai H, Nishimura K, Jiang N (2015) Enhanced thermal conductivity and retained electrical insulation for polyimide composites with SiC nanowires grown on graphene hybrid fillers. *Composites Part A* 76:73–81
303. Chen J, Chen X, Meng F, Li D, Tian X, Wang Z, Zhou Z (2017) Super-high thermal conductivity of polyamide-6/graphene-graphene oxide composites through in situ polymerization. *High Perform Polym* 29(5):585–594
304. Zong P, Fu J, Chen L, Yin J, Dong X, Yuan S, Shi L, Deng W (2016) Effect of aminopropylisobutyl polyhedral oligomeric silsesquioxane functionalized graphene on the thermal conductivity and electrical insulation properties of epoxy composites. *RSC Adv* 6(13):10498–10506
305. Ma W-S, Wu L, Yang F, Wang S-F (2014) Non-covalently modified reduced graphene oxide/polyurethane nanocomposites with good mechanical and thermal properties. *J Mater Sci* 49(2):562–571
306. Cho E-C, Huang J-H, Li C-P, Chang-Jian C-W, Lee K-C, Hsiao Y-S, Huang J-H (2016) Graphene-based thermoplastic composites and their application for LED thermal management. *Carbon* 102:66–73
307. Gojny FH, Wichmann MH, Fiedler B, Kinloch IA, Bauhofer W, Windle AH, Schulte K (2006) Evaluation and identification of electrical and thermal conduction mechanisms in carbon nanotube/epoxy composites. *Polymer* 47(6):2036–2045
308. Lee SH, Cho E, Jeon SH, Youn JR (2007) Rheological and electrical properties of polypropylene composites containing functionalized multi-walled carbon nanotubes and compatibilizers. *Carbon* 45(14):2810–2822
309. Kuilla T, Bhadra S, Yao D, Kim NH, Bose S, Lee JH (2010) Recent advances in graphene based polymer composites. *Prog Polym Sci* 35(11):1350–1375
310. Zhu J, Chen M, He Q, Shao L, Wei S, Guo Z (2013) An overview of the engineered graphene nanostructures and nanocomposites. *RSC Adv* 3(45):22790–22824
311. Zhu J, Wei S, Ryu J, Sun L, Luo Z, Guo Z (2010) Magnetic epoxy resin nanocomposites reinforced with core-shell structured Fe@FeO nanoparticles: fabrication and property analysis. *ACS Appl Mater Interfaces* 2(7):2100–2107
312. Moniruzzaman M, Winey KI (2006) Polymer nanocomposites containing carbon nanotubes. *Macromolecules* 39(16):5194–5205
313. Zhu J, Wei S, Ryu J, Budhathoki M, Liang G, Guo Z (2010) In situ stabilized carbon nanofiber (CNF) reinforced epoxy nanocomposites. *J Mater Chem* 20:4937–4948
314. Zhu J, Wei S, Yadav A, Guo Z (2010) Rheological behaviors and electrical conductivity of epoxy resin nanocomposites suspended with in-situ stabilized carbon nanofibers. *Polymer* 51(12):2643–2651
315. Zhu J, Wei S, Li Y, Sun L, Haldolaarachchige N, Young DP, Southworth C, Khasanov A, Luo Z, Guo Z (2011) Surfactant-free synthesized magnetic polypropylene nanocomposites: rheological, electrical, magnetic, and thermal properties. *Macromolecules* 44(11):4382–4391
316. Hu N, Fukunaga H, Atobe S, Liu Y, Li J (2011) Piezoresistive strain sensors made from carbon nanotubes based polymer nanocomposites. *Sensors* 11(11):10691–10723
317. Stankovich S, Dikin DA, Dommett GH, Kohlhaas KM, Zimney EJ, Stach EA, Piner RD, Nguyen ST, Ruoff RS (2006) Graphene-based composite materials. *Nature* 442(7100):282–286
318. Bryning MB, Islam MF, Kikkawa JM, Yodh AG (2005) Very low conductivity threshold in bulk isotropic single-walled carbon nanotube-epoxy composites. *Adv Mater* 17(9):1186–1191
319. Mamunya YP, Davydenko V, Pissis P, Lebedev E (2002) Electrical and thermal conductivity of polymers filled with metal powders. *Eur Polym J* 38(9):1887–1897
320. Song YS, Youn JR (2005) Influence of dispersion states of carbon nanotubes on physical properties of epoxy nanocomposites. *Carbon* 43(7):1378–1385

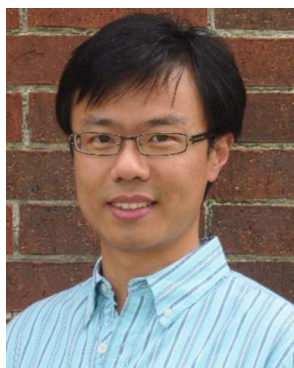
321. Barrau S, Demont P, Perez E, Peigney A, Laurent C, Lacabanne C (2003) Effect of palmitic acid on the electrical conductivity of carbon nanotubes–epoxy resin composites. *Macromolecules* 36(26):9678–9680
322. Sandler J, Kirk J, Kinloch I, Shaffer M, Windle A (2003) Ultra-low electrical percolation threshold in carbon-nanotube-epoxy composites. *Polymer* 44(19):5893–5899
323. Du F, Fischer JE, Winey KI (2005) Effect of nanotube alignment on percolation conductivity in carbon nanotube/polymer composites. *Phys Rev B* 72(12):121404
324. Sandler J, Kirk J, Kinloch I, Shaffer M, Windle A (2003) Ultra-low electrical percolation threshold in carbon-nanotube-epoxy composites. *Polymer* 44(19):5893–5899
325. Yu A, Ramesh P, Sun X, Bekyarova E, Itkis ME, Haddon RC (2008) Enhanced thermal conductivity in a hybrid graphite nanoplatelet–carbon nanotube filler for epoxy composites. *Adv Mater* 20(24):4740–4744
326. Sadasivuni KK, Ponnamma D, Kim J, Thomas S (2015) Graphene-based polymer nanocomposites in electronics. Springer International Publishing, New York
327. Stankovich S, Piner RD, Nguyen ST, Ruoff RS (2006) Synthesis and exfoliation of isocyanate-treated graphene oxide nanoplatelets. *Carbon* 44(15):3342–3347
328. Ramasubramanian R, Chen J, Liu H (2003) Homogeneous carbon nanotube/polymer composites for electrical applications. *Appl Phys Lett* 83(14):2928–2930
329. Ma L-F, Bao R-Y, Dou R, Zheng S-D, Liu Z-Y, Zhang R-Y, Yang M-B, Yang W (2016) Conductive thermoplastic vulcanizates (TPVs) based on polypropylene (PP)/ethylene-propylene-diene rubber (EPDM) blend: from strain sensor to highly stretchable conductor. *Compos Sci Technol* 128:176–184
330. Du F-P, Tang H, Huang D-Y (2013) Thermal conductivity of epoxy resin reinforced with magnesium oxide coated multiwalled carbon nanotubes. *Int J Polym Sci* 541823:1–5
331. Karim MR, Lee CJ, Chowdhury AS, Nahar N, Lee MS (2007) Radiolytic synthesis of conducting polypyrrole/carbon nanotube composites. *Mater Lett* 61(8):1688–1692
332. Dang ZM, Wang L, Yin Y, Zhang Q, Lei QQ (2007) Giant dielectric permittivities in functionalized carbon-nanotube/electroactive-polymer nanocomposites. *Adv Mater* 19(6):852–857
333. Kwon JY, Kim HD (2005) Preparation and properties of acid-treated multiwalled carbon nanotube/waterborne polyurethane nanocomposites. *J Appl Polym Sci* 96(2):595–604
334. Kim H-S, Park BH, Yoon J-S, Jin H-J (2007) Nylon 610/functionalized multiwalled carbon nanotubes composites by in situ interfacial polymerization. *Mater Lett* 61(11):2251–2254
335. Karim MR, Lee CJ, Lee MS (2006) Synthesis and characterization of conducting polythiophene/carbon nanotubes composites. *J Polym Sci Part A Polym Chem*. 44(18):5283–5290
336. Kuila BK, Malik S, Batabyal SK, Nandi AK (2007) In-situ synthesis of soluble poly (3-hexylthiophene)/multiwalled carbon nanotube composite: morphology, structure, and conductivity. *Macromolecules* 40(2):278–287
337. Long Y, Chen Z, Zhang X, Zhang J, Liu Z (2004) Synthesis and electrical properties of carbon nanotube polyaniline composites. *Ppl Phys Lett* 85(10):1796–1798
338. Chen J, Ramasubramanian R, Xue C, Liu H (2006) A versatile, molecular engineering approach to simultaneously enhanced, multifunctional carbon-nanotube–polymer composites. *Adv Funct Mater* 16(1):114–119
339. Kim KH, Jo WH (2009) A strategy for enhancement of mechanical and electrical properties of polycarbonate/multi-walled carbon nanotube composites. *Carbon* 47(4):1126–1134



search is on selective enhancement of thermal properties of polymeric materials and composites.



Nitin Mehra received his Bachelors and Masters both in Chemical Engineering from the Indian Institute of Technology Bombay (IIT), India. Currently, he is a Ph.D. student in the Department of Chemical and Biomolecular Engineering at The University of Akron. His research interests lie in understanding the principles governing thermal conduction in polymer-based materials with particular focus on thermally conductive polymer composites for heat management applications.



Dr. Jiahua Zhu is an Assistant Professor in the Department of Chemical & Biomolecular Engineering at The University of Akron. Dr. Zhu received his Ph.D. degree of Chemical Engineering from Lamar University in 2013. Dr. Zhu's current research interest covers the fundamental study of multifunctional polymer- and carbon-based nanocomposites and explores their applications in emerging fields such as heat transport, energy storage, catalysis, and environmental remediation. Dr. Zhu was awarded the Young Leader Development Award from the Functional Material Division of The Minerals, Metals & Materials Society, the Early Career Award from the Polymer Processing Society, and the Early Career Investigator Award from the ECS Electrodeposition Division.